Appendices

A Maximal dynamic range of real signals

Since the selection of a window function involves a trade-off between spectral leakage (i.e. how well the sidelobes are suppressed compared with the main peak) and bandwidth, it is interesting to investigate what maximal dynamic range we can expect from real signals. We consider here two common noise sources that limit the dynamic range: electronic noise and digitizing noise. The aim is to use window functions that do not deteriorate the noise floor originating from these inevitable noise sources, i.e. the spectral leakage of the window transfer function at a reasonable frequency separation should be considerably lower (e.g. at least 6 dB) than the inherent dynamic range of the input signal. This requirement is, of course, rather vague, and the answer depends on the characteristics of the particular input signal in question.

A.1 Electronic noise

All signals fed to an A/D converter must first pass through various electronic circuits which have a certain noise level. To find a lower limit for that noise, we consider as example an ultra-low-noise operational amplifier (such as AD797 or LT1028). These amplifiers typically have a useful signal range of approximately $\pm 12\,\mathrm{V}$, and an input noise level[5] of approximately $2\,\mathrm{nV}/\sqrt{\mathrm{Hz}}$. In order to compute the dynamic range we compare the maximal amplitude of a sinusoidal signal

$$U_{\max} = 12\,\mathrm{V_{pk}} \approx 8.5\,\mathrm{V_{rms}}\,, \tag{30}$$

with the noise accumulated in one frequency bin

$$U_{\mathrm{noise}} = 2\,\frac{\mathrm{nV_{rms}}}{\sqrt{\mathrm{Hz}}} \cdot \sqrt{\mathrm{ENBW}}\,. \tag{31}$$

For the comparison we have to specify the noise bandwidth ENBW given by

$$\mathrm{ENBW} = \mathrm{NENBW} \cdot f_{\mathrm{res}}\,, \tag{32}$$

where f_{res} is the width of one frequency bin, and NENBW is in the range $1\ldots4$, depending on the window function (see Equation (22)). The comparison is shown in Figure 12. If the dynamic range were limited by electronic noise alone, the requirements on the dynamic range of the window function would be rather stringent.

A.2 Digitizing noise

The noise source that usually limits the dynamic range of spectrum measurements is caused by the digitizing process introducing a noise linear spectral density given by

$$\widetilde{U}_{\mathrm{dig}} = \frac{U_{\mathrm{LSB}}}{\sqrt{6 \cdot f_{\mathrm{s}}}}\,, \tag{33}$$

[5]The input *voltage* noise of these amplifiers is approximately $1\,\mathrm{nV}/\sqrt{\mathrm{Hz}}$, but in any real application we have additional noise contributions from the thermal noise of the input impedance and the input current noise.

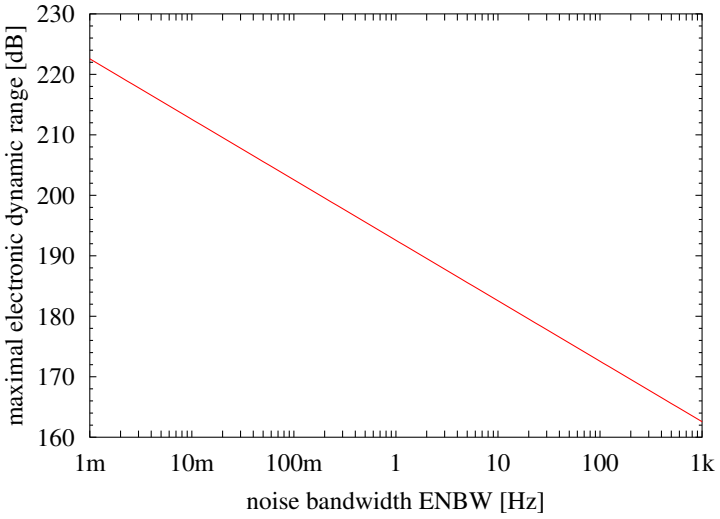

Figure 12 *Maximal dynamic range of electronic signals, assuming a range of* $\pm 12\,V$ *and an input noise level of* $2\,nV/\sqrt{\text{Hz}}$.

where U_{LSB} is the voltage corresponding to one least significant bit and f_s the sampling frequency (see e.g. Reference [Lyons, Section 9.3]). We assume using an A/D converter with an effective resolution[6] of n bits. The maximal amplitude of a sinusoidal signal is then given by

$$U_{\text{max, pk}} = 2^{n-1} \cdot U_{\text{LSB}}\,, \tag{34}$$

$$U_{\text{max, rms}} = \frac{2^{n-1}}{\sqrt{2}}\, U_{\text{LSB}}\,, \tag{35}$$

which we have to compare with the noise accumulated in one frequency bin

$$U_{\text{noise, rms}} = \widetilde{U}_{\text{dig}} \cdot \sqrt{\text{ENBW}} \tag{36}$$

$$= \frac{U_{\text{LSB}}}{\sqrt{6 \cdot f_s}} \cdot \sqrt{\text{NENBW} \cdot f_{\text{res}}} \tag{37}$$

$$= U_{\text{LSB}} \cdot \sqrt{\frac{\text{NENBW}}{6\,N}}\,, \tag{38}$$

where N is the length of the DFT. The dynamic range is hence given by

$$\frac{U_{\text{max, rms}}}{U_{\text{noise, rms}}} = 2^{n-1} \cdot \sqrt{N} \cdot \sqrt{\frac{3}{\text{NENBW}}}\,. \tag{39}$$

This function is shown in Figure 13 for a typical value of NENBW = 3 bins and several values of the A/D resolution n. Since the effective resolution of modern A/D converters reaches 20 bits or better, we may expect a dynamic range of up to 180 dB under optimal conditions. In practice,

[6]The effective resolution of an A/D converter is always smaller than its nominal resolution due to imperfections and noise. On the other hand, the effective resolution can be enhanced to a value that is better than the nominal resolution by averaging several samples. Indeed one standard method to evaluate the effective resolution of an A/D converter is to digitize a known sine wave, compute a spectrum with a DFT, determine the noise floor and evaluate Equation (33).

other noise sources (such as those originating in the experiment itself, e.g. technical noise, shot noise etc.) are often likely to have a noise level higher than the digitizing noise. Hence in many cases the window functions available in the past (e.g. Hanning, Nuttall, or Salvatore's flat-top windows) have a sufficient dynamic range such as not to introduce additional noise above the noise floor that is present anyway. In favourable conditions, however, the dynamic range of those window functions is worse than the dynamic range of the rest of the signal chain, in particular in the case of flat-top windows, which had been limited to a sidelobe level of −90 dB so far. Then the new flat-top window functions introduced in this paper, having a much better dynamic range, become attractive.

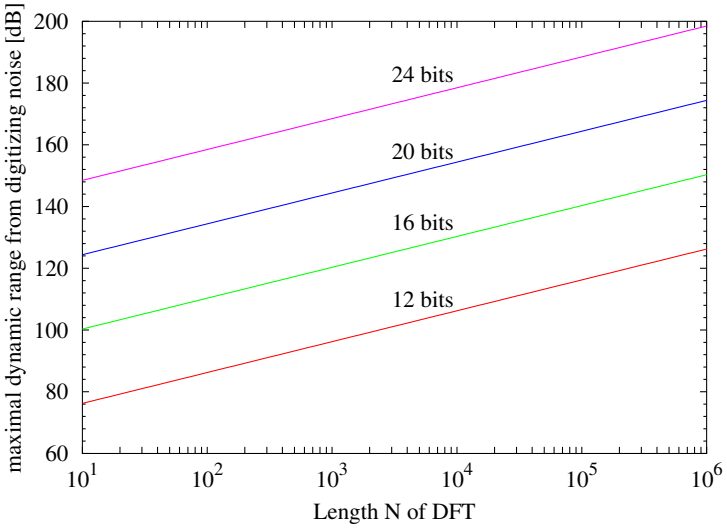

Figure 13 *Maximal dynamic range due to digitizing noise, computed for NENBW=3 bins.*

B Computing the response of a window function

The response $a(f)$ of a window for a frequency offset of f bins can be computed as follows:

$$a_\mathrm{r}(f) = \sum_{j=0}^{N-1} w_j \cos(2\pi f\, j/N)\,, \quad \text{(real part)} \tag{40}$$

$$a_\mathrm{i}(f) = \sum_{j=0}^{N-1} w_j \sin(2\pi f\, j/N)\,, \quad \text{(imaginary part)} \tag{41}$$

$$a(f) = \frac{\sqrt{a_\mathrm{r}^2 + a_\mathrm{i}^2}}{S_1}. \tag{42}$$

Using the symmetry of the window coefficients (Equation (18)) and some trigonometric relations $a(f)$ can be computed more efficiently as follows:

$$a_0(f) = w_{N/2} + 2 \sum_{j=1}^{N/2-1} w_j \cos\left(\pi f \left[\frac{2j}{N} - 1\right]\right), \tag{43}$$

$$a_\mathrm{r}(f) = w_0 + \cos(\pi f)\, a_0(f), \tag{44}$$

$$a_\mathrm{i}(f) = \sin(\pi f)\, a_0(f), \tag{45}$$

$$a(f) = \frac{\sqrt{a_\mathrm{r}^2 + a_\mathrm{i}^2}}{S_1}. \tag{46}$$

For the common case $w_0 = 0$ this can be further simplified:

$$a(f) = a_0(f)/S_1. \tag{47}$$

In the case of windows that are defined as a sum of m cosine terms:

$$w_j = 1 + \sum_{k=1}^{m} c_k \cos k\frac{2\pi\, j}{N}, \tag{48}$$

the transfer function can be computed directly, without fixing a finite number N of samples, and very efficiently as a sum of shifted Dirichlet kernels:

$$x(f) = \frac{1}{f} + \frac{1}{2}\sum_{k=1}^{m} c_k \left(\frac{1}{f+k} + \frac{1}{f-k}\right), \tag{49}$$

$$a_\mathrm{r}(f) = \sin(2\pi f)\, \frac{x(f)}{2\pi}, \tag{50}$$

$$a_\mathrm{i}(f) = (1 - \cos(2\pi f))\, \frac{x(f)}{2\pi}, \tag{51}$$

$$a(f) = \sqrt{a_\mathrm{r}^2 + a_\mathrm{i}^2}\,, \tag{52}$$

for frequency offsets $f \neq 0$, and $a(0) = 1$. If f falls on an exact integer k, the above expression reduces to

$$a(f) = |c_k|/2\,. \tag{53}$$

Incidentially, the normalized equivalent noise bandwidth NENBW can also be computed directly for windows of the form (48):

$$\mathrm{NENBW} = 1 + \frac{1}{2}\sum_{k=1}^{m} c_k^2\,. \tag{54}$$

C List of window functions

This appendix lists many popular and useful window functions, including several new high-performance functions recently developed by one of the authors (G.H.). Each window function is described in a text section below and graphically shown on a seperate page at the end of this document. Furthermore, Table 2 summarizes the main characteristics of each window.

Name	Text Section	Graph page	PSLL [dB]	SLDR [f^{-n}]	NENBW [bins]	3 dB BW [bins]	flatness [dB]	ROV [%]
Rectangular	C.1 p.30	51	13.3	1	1.0000	0.8845	−3.9224	0.0
Welch	C.3 p.31	53	21.3	2	1.2000	1.1535	−2.2248	29.3
Bartlett	C.2 p.30	52	26.5	2	1.3333	1.2736	−1.8242	50.0
Hanning	C.4 p.31	54	31.5	3	1.5000	1.4382	−1.4236	50.0
Hamming	C.5 p.32	55	42.7	1	1.3628	1.3008	−1.7514	50.0
Nuttall3	C.7.1 p.34	57	46.7	5	1.9444	1.8496	−0.8630	64.7
Nuttall4	C.7.4 p.35	60	60.9	7	2.3100	2.1884	−0.6184	70.5
Nuttall3a	C.7.2 p.35	58	64.2	3	1.7721	1.6828	−1.0453	61.2
Kaiser3	C.8 p.36	64	69.6	1	1.7952	1.7025	−1.0226	61.9
Nuttall3b	C.7.3 p.35	59	71.5	1	1.7037	1.6162	−1.1352	59.8
Nuttall4a	C.7.5 p.35	61	82.6	5	2.1253	2.0123	−0.7321	68.0
BH92	C.6 p.32	56	92.0	1	2.0044	1.8962	−0.8256	66.1
Nuttall4b	C.7.6 p.36	62	93.3	3	2.0212	1.9122	−0.8118	66.3
Kaiser4	C.8 p.36	65	94.4	1	2.0533	1.9417	−0.7877	67.0
Nuttall4c	C.7.7 p.36	63	98.1	1	1.9761	1.8687	−0.8506	65.6
Kaiser5	C.8 p.36	66	119.8	1	2.2830	2.1553	−0.6403	70.5
Flat-top windows:								
SFT3F	D.1.1 p.40	67	31.7	3	3.1681	3.1502	+0.0082	66.7
SFT3M	D.1.4 p.41	70	44.2	1	2.9452	2.9183	−0.0115	65.5
FTNI	D.2.1 p.42	73	44.4	1	2.9656	2.9355	+0.0169	65.6
SFT4F	D.1.2 p.40	68	44.7	5	3.7970	3.7618	+0.0041	75.0
SFT5F	D.1.3 p.40	69	57.3	7	4.3412	4.2910	−0.0025	78.5
SFT4M	D.1.5 p.41	71	66.5	1	3.3868	3.3451	−0.0067	72.1
FTHP	D.2.2 p.42	74	70.4	1	3.4279	3.3846	+0.0096	72.3
HFT70	D.3.1 p.45	76	70.4	1	3.4129	3.3720	−0.0065	72.2
FTSRS	D.2.4 p.43	75	76.6	3	3.7702	3.7274	−0.0156	75.4
SFT5M	D.1.6 p.41	72	89.9	1	3.8852	3.8340	+0.0039	76.0
HFT90D	D.3.3 p.46	78	90.2	3	3.8832	3.8320	−0.0039	76.0
HFT95	D.3.2 p.46	77	95.0	1	3.8112	3.7590	+0.0044	75.6
HFT116D	D.3.4 p.47	79	116.8	3	4.2186	4.1579	−0.0028	78.2
HFT144D	D.3.5 p.47	80	144.1	3	4.5386	4.4697	+0.0021	79.9
HFT169D	D.3.6 p.47	81	169.5	3	4.8347	4.7588	+0.0017	81.2
HFT196D	D.3.7 p.48	82	196.2	3	5.1134	5.0308	+0.0013	82.3
HFT223D	D.3.8 p.48	83	223.0	3	5.3888	5.3000	−0.0011	83.3
HFT248D	D.3.9 p.49	84	248.4	3	5.6512	5.5567	+0.0009	84.1

Table 2 *Summary of important characteristics of each window function discussed in this report. PSLL='peak sidelobe level', SLDR='sidelobe drop rate', NENBW='normalized equivalent noise bandwidth', ROV='recommended overlap'.*

C.1 Rectangular window

The rectangular window, also sometimes called 'uniform window', is given by

$$w_j \equiv 1, \tag{55}$$

i.e. equivalent to using no window at all. Its transfer function and characteristic bandwidths are shown in Figure 15 on page 51 and are given by

$$\text{NENBW} = 1.0000\,\text{bins}\,, \tag{56}$$
$$W_{3\,\text{dB}} = 0.8845\,\text{bins}\,, \tag{57}$$
$$e_{\max} = -3.9224\,\text{dB} = -36.3380\,\%. \tag{58}$$

The first zero is located at $f = \pm 1.00$ bins. The highest sidelobe is $-13.3\,\text{dB}$, located at $f = \pm 1.43$ bins. The sidelobes drop at a rate of f^{-1}. Overlapping makes no sense for the Rectangular window.

While $W_{3\,\text{dB}}$ is the narrowest of all windows, $e_{\max}$ and the spectral leakage are the worst of all windows considered here. Although there are some special applications where the rectangular window is advantageous, it is probably not useful for any of our applications in GEO 600 and mentioned here mainly for completeness.

C.2 Bartlett window

The Bartlett window is described, e.g., in Reference [Harris78] and given by

$$z = \frac{2 \cdot j}{N}, \quad j = 0 \ldots N-1, \tag{59}$$
$$w_j = \begin{cases} z; & z \leq 1, \\ 2 - z; & z > 1, \end{cases} \tag{60}$$

i.e. a triangular function. Its transfer function and characteristics are shown in Figure 16 on page 52 and are given by

$$\text{NENBW} = 1.3333\,\text{bins}\,, \tag{61}$$
$$W_{3\,\text{dB}} = 1.2736\,\text{bins}\,, \tag{62}$$
$$e_{\max} = -1.8242\,\text{dB} = -18.9430\,\%. \tag{63}$$

The first zero is located at $f = \pm 2.00$ bins. The highest sidelobe is $-26.5\,\text{dB}$, located at $f = \pm 2.86$ bins. The sidelobes drop at a rate of f^{-2}. At the optimal overlap of 50.0%, the amplitude flatness is 1.000, the power flatness is 0.707, and the overlap correlation is 0.250 .

The Bartlett window offers a narrow bandwidth and might be useful in situations where the amplitude accuracy is unimportant and the relatively high first sidelobe does not disturb. In most situations, however, the Bartlett window does not offer any particular advantage compared with the more sophisticated windows described below and is mentioned here mainly for completeness.

C.3 Welch window

The Welch window is described, e.g., in Reference [Harris78] and given by

$$z = \frac{2 \cdot j}{N}, \quad j = 0 \ldots N-1, \tag{64}$$

$$w_j = 1 - (z-1)^2\,; \tag{65}$$

i.e. a parabolic function. Its transfer function and characteristics are shown in Figure 17 on page 53 and are given by

$$\mathrm{NENBW} = 1.2000\,\mathrm{bins}\,, \tag{66}$$

$$W_{3\,\mathrm{dB}} = 1.1535\,\mathrm{bins}\,, \tag{67}$$

$$e_{\max} = -2.2248\,\mathrm{dB} = -22.5962\,\%. \tag{68}$$

The first zero is located at $f = \pm 1.43$ bins. The highest sidelobe is $-21.3\,\mathrm{dB}$, located at $f = \pm 1.83$ bins. The sidelobes drop at a rate of f^{-2}. At the optimal overlap of 29.3%, the amplitude flatness is 0.828, the power flatness is 0.707, and the overlap correlation is 0.091 .

The Welch window offers a narrow bandwidth and might be useful in situations where the amplitude accuracy is unimportant and the relatively high first sidelobe does not disturb. In most situations, however, the Welch window does not offer any particular advantage compared with the more sophisticated windows described below and is mentioned here mainly for completeness.

C.4 Hanning window

The Hanning window (one of a family of 'raised cosine' windows) is also known as 'Hann window'. According to Reference [Harris78], it is named after the Austrian meteorologist Julius von Hann. Do not confuse it with the 'Hamming' window (see Section C.5). The Hanning window has already been used as example in Section 8, its properties are summarized here again for completeness. It is described, e.g., in Reference [Harris78] and given by

$$z = \frac{2\pi \cdot j}{N}, \quad j = 0 \ldots N-1, \tag{69}$$

$$w_j = \frac{1 - \cos(z)}{2} = \cos^2\left(\frac{z-\pi}{2}\right); \tag{70}$$

i.e. part of a cosine function. Its transfer function and characteristics are shown in Figure 18 on page 54 and are given by

$$\mathrm{NENBW} = 1.5000\,\mathrm{bins}\,, \tag{71}$$

$$W_{3\,\mathrm{dB}} = 1.4382\,\mathrm{bins}\,, \tag{72}$$

$$e_{\max} = -1.4236\,\mathrm{dB} = -15.1174\,\%. \tag{73}$$

The first zero is located at $f = \pm 2.00$ bins. The highest sidelobe is $-31.5\,\mathrm{dB}$, located at $f = \pm 2.36$ bins. The sidelobes drop at a rate of f^{-3}. At the optimal overlap of 50.0%, the amplitude flatness is 1.000, the power flatness is 0.707, and the overlap correlation is 0.167 .

The Hanning window has reasonably low spectral leakage and bandwidth and is hence used as standard window function in many commercial spectrum analyzers, if amplitude accuracy for sinusoidal signals is not important (i.e. in noise measurements).

C.5 Hamming window

The Hamming window is the simplest example of a family of windows that are constructed as a weighted sum of a constant term and some cosine terms. Do not confuse it with the 'Hanning' window (see Section C.4). The Hamming window is given by

$$z = \frac{2\pi \cdot j}{N}, \quad j = 0 \ldots N-1, \tag{74}$$

$$w_j = 0.54 - 0.46\,\cos(z); \tag{75}$$

The coefficients are chosen such that the first sidelobe becomes nearly minimal.[7] There is discontinuity of 0.08 at the boundary, leading to a sidelobe-drop rate of only f^{-1}. The transfer function and characteristics are shown in Figure 19 on page 55 and are given by

$$\mathrm{NENBW} = 1.3628\,\mathrm{bins}\,, \tag{76}$$

$$W_{3\,\mathrm{dB}} = 1.3008\,\mathrm{bins}\,, \tag{77}$$

$$e_{\max} = -1.7514\,\mathrm{dB} = -18.2612\,\%. \tag{78}$$

The first zero is located at $f = \pm 2.00$ bins. The highest sidelobe is -42.7 dB, located at $f = \pm 4.50$ bins. At the optimal overlap of 50.0%, the amplitude flatness is 1.000, the power flatness is 0.761, and the overlap correlation is 0.234 . The last graph in Figure 19 on page 55 shows some discontinuities in the 'amplitude flatness (AF)' curve. These originate from the discontinuity at the boundary in the time domain. If, for an overlap of 50 %, two instances of the window are exactly adjacent to each other without any gap, the resulting summed amplitude becomes perfectly flat (similar to the Hanning window for 50 % overlap), and the amplitude flatness reaches unity. A gap or overlap of only one sample in the time domain, however, causes a dip or peak in the summed amplitude, which results in an amplitude flatness of less than unity.

The Hamming window offers a narrow bandwidth and might be useful in situations where the amplitude accuracy is unimportant and the slow dropping rate of the sidelobes does not disturb.

C.6 Blackman-Harris window

The Blackman-Harris window is one of a family of window functions given by a sum of cosine terms. By varying the number and coefficients of the terms different characteristics can be optimized. The window we describe here is called 'minimum 4-term Blackman-Harris window' and was designed to have a small sidelobe adjacent to the main peak in the transfer function. Because the highest sidelobe is 92 dB below the main peak, it is also called '92 dB Blackman-Harris window' to distinguish it from other members of that family. In this report its name is also abbreviated as 'BH92'. It is described in [Harris78] and given by

$$z = \frac{2\pi \cdot j}{N}, \quad j = 0 \ldots N-1, \tag{79}$$

$$w_j = 0.35875 - 0.48829\cos(z) + 0.14128\cos(2z) - 0.01168\cos(3z). \tag{80}$$

Its transfer function and characteristics are shown in Figure 20 on page 56 and are given by

$$\mathrm{NENBW} = 2.0044\,\mathrm{bins}\,, \tag{81}$$

$$W_{3\,\mathrm{dB}} = 1.8962\,\mathrm{bins}\,, \tag{82}$$

$$e_{\max} = -0.8256\,\mathrm{dB} = -9.0670\,\%. \tag{83}$$

[7] The minimal sidelobe level that can be reached with this form of function is -43.2 dB for a window given by $0.538379 - 0.461621\cos(z)$.

The first zero is located at $f = \pm 4.00$ bins. The highest sidelobe is $-92.0\,\mathrm{dB}$, located at $f = \pm 4.52$ bins. The sidelobes drop at a rate of f^{-1}. At the optimal overlap of 66.1%, the amplitude flatness is 0.926, the power flatness is 0.718, and the overlap correlation is 0.235 .

The Blackman-Harris window has very low spectral leakage combined with reasonable bandwidth and amplitude error. Due to its small sidelobes it is suitable for the detection of small sinusoidal signals adjacent in frequency to large signals. It can also be used as a general-purpose window in applications with high dynamic range if amplitude accuracy for sinusoidal signals is not very important. Note, however, that two of the Nuttall windows (called 'Nuttall4b' and 'Nuttall4c', see next Section C.7) have even lower sidelobes with the same number of cosine terms and otherwise comparable properties.

C.7 Nuttall windows

These windows are defined as a weighted sum of cosine terms (as are the Hanning, Hamming, Blackman-Harris and flat-top windows):

$$z = \frac{2\pi \cdot j}{N}, \quad j = 0 \ldots N-1, \tag{84}$$

$$w_j = \sum_{k=0}^{m} c_k \cos(k \cdot z) = c_0 + \sum_{k=1}^{m} c_k \cos(k \cdot z). \tag{85}$$

Nuttall gives several sets of coefficients $\{c_k\}$ in his paper [Nuttall81], which are optimized for different aims. The coefficients are summarized in Table 3.

Name	c_0	c_1	c_2	c_3	SLDR f^{-n}	PSLL [dB]	Graph page
Nuttall3	0.375	−0.5	0.125	0	5	−46.7	57
Nuttall3a	0.40897	−0.5	0.09103	0	3	−64.2	58
Nuttall3b	0.4243801	−0.4973406	0.0782793	0	1	−71.5	59
Nuttall4	0.3125	−0.46875	0.1875	−0.03125	7	−60.9	60
Nuttall4a	0.338946	−0.481973	0.161054	−0.018027	5	−82.6	61
Nuttall4b	0.355768	−0.487396	0.144232	−0.012604	3	−93.3	62
Nuttall4c	0.3635819	−0.4891775	0.1365995	−0.0106411	1	−98.1	63

Table 3 *Coefficients of Nuttall window functions, to be used with Equation (85).*

In designing these window functions, a trade-off has been made between the dropping rate of the sidelobes (SLDR) and the maximal sidelobe level. After first selecting the number of terms (e.g. the window functions named Nuttall3 have 3 terms: one constant term and two cosine terms) one fixes the degree of differentiability of the window function at its boundary.

For functions of the form (85) it turns out that each extra condition on the coefficients is enough to make the function twice more differentiable, i.e. the condition

$$\sum_{k=0}^{m} c_k = 0 \tag{86}$$

ensures that the function is continuous at the boundary but at the same time implies that it is also differentiable once and hence has a SLDR of f^{-3}. A function that does not fulfill Equation (86) is discontinuous at the boundary and has a SLDR of f^{-1} only.

Similarly, the condition

$$\sum_{k=0}^{m} k^2 \, c_k = 0 \tag{87}$$

ensures not only twice, but also three times differentiability and hence results in a SLDR of f^{-5}, while

$$\sum_{k=0}^{m} k^4 \, c_k = 0 \tag{88}$$

yields a SLDR of f^{-7} etc.

The window functions called 'Nuttall3' and 'Nuttall4' are chosen such as to have the maximum possible degree of differentiability for a given number of terms. After fixing an arbitrary common factor[8], there are two or three degrees of freedom available in the 'Nuttall3' and 'Nuttall4' family of windows, respectively. The subsequent functions called 'a', 'b', etc., relax the differentiability requirement by one level each and use the degrees of freedom thus becoming available to minimize the peak sidelobe level (PSLL).

The 'Nuttall2' window, i.e. one cosine term chosen for maximal differentiability, is just the Hanning window, while the window that might be called 'Nuttall2a' (minimal PSLL) would be the Hamming window.

The Nuttall windows, especially 'Nuttall3b', 'Nuttall4b' and 'Nuttall4c', have very low spectral leakage combined with reasonable bandwidth and amplitude error. Due to their small sidelobes they are suitable for the detection of small sinusoidal signals adjacent in frequency to large signals. They can also be used as a general-purpose window in applications with high dynamic range if amplitude accuracy for sinusoidal signals is not very important.

C.7.1 Nuttall3

The window called 'Nuttall3' is derived by requiring the maximal possible SLDR of f^{-5} for a three-term function. Its coefficients are taken from Ref. [Nuttall81] and listed in Table 3. The function is identical to $\cos^4(\pi(j/N - 1/2))$. The transfer function and characteristics are shown in Figure 21 and are given by

$$\text{NENBW} = 1.9444\,\text{bins}\,, \tag{89}$$

$$W_{3\,\text{dB}} = 1.8496\,\text{bins}\,, \tag{90}$$

$$e_{\max} = -0.8630\,\text{dB} = -9.4585\,\%. \tag{91}$$

The first zero is located at $f = \pm 3.00$ bins. The highest sidelobe is -46.7 dB, located at $f = \pm 3.33$ bins. At the optimal overlap of 64.7%, the amplitude flatness is 0.969, the power flatness is 0.738, and the overlap correlation is 0.228 .

[8] Nuttall chose the condition $\sum(-1)^k c_k = 1$ which corresponds to normalizing the value of the window function in the center to unity: $w_{N/2} = 1$.

C.7.2 Nuttall3a

The window called 'Nuttall3a' is derived by requiring a SLDR of f^{-3} for a three-term function and using the remaining degree of freedom to minimize the PSLL. Its coefficients are taken from Ref. [Nuttall81] and listed in Table 3. The transfer function and characteristics are shown in Figure 22 and are given by

$$\text{NENBW} = 1.7721\,\text{bins}\,, \tag{92}$$
$$W_{3\,\text{dB}} = 1.6828\,\text{bins}\,, \tag{93}$$
$$e_{\max} = -1.0453\,\text{dB} = -11.3387\,\%. \tag{94}$$

The first zero is located at $f = \pm 3.00$ bins. The highest sidelobe is -64.2 dB, located at $f = \pm 4.49$ bins. At the optimal overlap of 61.2%, the amplitude flatness is 0.943, the power flatness is 0.723, and the overlap correlation is 0.227 .

C.7.3 Nuttall3b

The window called 'Nuttall3b' is derived by using the two degrees of freedom in a three-term function to minimize the PSLL. Its coefficients are taken from Ref. [Nuttall81] and listed in Table 3. The transfer function and characteristics are shown in Figure 23 and are given by

$$\text{NENBW} = 1.7037\,\text{bins}\,, \tag{95}$$
$$W_{3\,\text{dB}} = 1.6162\,\text{bins}\,, \tag{96}$$
$$e_{\max} = -1.1352\,\text{dB} = -12.2519\,\%. \tag{97}$$

The first zero is located at $f = \pm 3.00$ bins. The highest sidelobe is -71.5 dB, located at $f = \pm 3.64$ bins. At the optimal overlap of 59.8%, the amplitude flatness is 0.939, the power flatness is 0.721, and the overlap correlation is 0.229 .

C.7.4 Nuttall4

The window called 'Nuttall4' is derived by requiring the maximal possible SLDR of f^{-7} for a four-term function. Its coefficients are taken from Ref. [Nuttall81] and listed in Table 3. The function is identical to $\cos^6(\pi(j/N - 1/2))$. The transfer function and characteristics are shown in Figure 24 and are given by

$$\text{NENBW} = 2.3100\,\text{bins}\,, \tag{98}$$
$$W_{3\,\text{dB}} = 2.1884\,\text{bins}\,, \tag{99}$$
$$e_{\max} = -0.6184\,\text{dB} = -6.8716\,\%. \tag{100}$$

The first zero is located at $f = \pm 4.00$ bins. The highest sidelobe is -60.9 dB, located at $f = \pm 4.30$ bins. At the optimal overlap of 70.5%, the amplitude flatness is 0.937, the power flatness is 0.723, and the overlap correlation is 0.233 .

C.7.5 Nuttall4a

The window called 'Nuttall4a' is derived by requiring a SLDR of f^{-5} for a four-term function and using the remaining degree of freedom to minimize the PSLL. Its coefficients are taken from

Ref. [Nuttall81] and listed in Table 3. The transfer function and characteristics are shown in Figure 25 and are given by

$$\text{NENBW} = 2.1253\,\text{bins}\,, \tag{101}$$

$$W_{3\,\text{dB}} = 2.0123\,\text{bins}\,, \tag{102}$$

$$e_{\max} = -0.7321\,\text{dB} = -8.0827\,\%. \tag{103}$$

The first zero is located at $f = \pm 4.00$ bins. The highest sidelobe is $-82.6\,\text{dB}$, located at $f = \pm 5.45$ bins. At the optimal overlap of 68.0%, the amplitude flatness is 0.931, the power flatness is 0.721, and the overlap correlation is 0.234 .

C.7.6 Nuttall4b

The window called 'Nuttall4b' is derived by requiring a SLDR of f^{-3} for a four-term function and using the remaining two degrees of freedom to minimize the PSLL. Its coefficients are taken from Ref. [Nuttall81] and given in Table 3. The transfer function and characteristics are shown in Figure 26 and are given by

$$\text{NENBW} = 2.0212\,\text{bins}\,, \tag{104}$$

$$W_{3\,\text{dB}} = 1.9122\,\text{bins}\,, \tag{105}$$

$$e_{\max} = -0.8118\,\text{dB} = -8.9223\,\%. \tag{106}$$

The first zero is located at $f = \pm 4.00$ bins. The highest sidelobe is $-93.3\,\text{dB}$, located at $f = \pm 4.57$ bins. At the optimal overlap of 66.3%, the amplitude flatness is 0.924, the power flatness is 0.715, and the overlap correlation is 0.233 .

C.7.7 Nuttall4c

The window called 'Nuttall4c' is derived by using all three degrees of freedom in a four-term function to minimize the PSLL. Its coefficients are taken from Ref. [Nuttall81] and listed in Table 3. The transfer function and characteristics are shown in Figure 26 and are given by

$$\text{NENBW} = 1.9761\,\text{bins}\,, \tag{107}$$

$$W_{3\,\text{dB}} = 1.8687\,\text{bins}\,, \tag{108}$$

$$e_{\max} = -0.8506\,\text{dB} = -9.3282\,\%. \tag{109}$$

The first zero is located at $f = \pm 4.00$ bins. The highest sidelobe is $-98.1\,\text{dB}$, located at $f = \pm 6.48$ bins. At the optimal overlap of 65.6%, the amplitude flatness is 0.923, the power flatness is 0.716, and the overlap correlation is 0.235 .

C.8 Kaiser window

The Kaiser window (also called Kaiser-Bessel window) is derived by maximizing, in a certain sense, the energy that falls in the main peak of the transfer function. It is defined by (see, e.g., Reference [Harris78]):

$$z = \frac{2 \cdot j}{N} - 1, \quad j = 0 \ldots N-1, \tag{110}$$

$$w_j = \frac{I_0\left(\pi\alpha\sqrt{1-z^2}\right)}{I_0\left(\pi\alpha\right)}; \tag{111}$$

α	PSLL [dB]	NENBW [bins]	3 dB BW [bins]	zero [bins]	flatness [dB]	ROV [%]
2.0	−45.9	1.4963	1.4270	2.24	−1.4527	53.4
2.5	−57.6	1.6519	1.5700	2.69	−1.2010	58.3
3.0	−69.6	1.7952	1.7025	3.16	−1.0226	61.9
3.5	−81.9	1.9284	1.8262	3.64	−0.8900	64.7
4.0	−94.4	2.0533	1.9417	4.12	−0.7877	67.0
4.5	−107.0	2.1712	2.0512	4.61	−0.7064	68.9
5.0	−119.8	2.2830	2.1553	5.10	−0.6403	70.5
5.5	−132.6	2.3898	2.2546	5.59	−0.5854	71.9
6.0	−145.5	2.4920	2.3499	6.08	−0.5392	73.1
6.5	−158.4	2.5902	2.4414	6.58	−0.4998	74.1
7.0	−171.4	2.6848	2.5297	7.07	−0.4657	75.1

Table 4 *Summary of important characteristics of the Kaiser window for some values of the parameter α. PSLL='peak sidelobe level', NENBW='normalized equivalent noise bandwidth', 'zero'='location of first zero', ROV='recommended overlap'.*

where I_0 is the zero-order modified Bessel function of the first kind:

$$I_0(x) = \sum_{k=0}^{\infty} \left[\frac{(x/2)^k}{k!} \right]^2 , \tag{112}$$

and α is a parameter that parameterizes a trade-off between the sidelobe level and the width of the central peak. Typical values are in the range 2 to 5. The Kaiser window has a small but finite discontinuity at the boundary and hence its sidelobes drop only as f^{-1}, although the initial sidelobe level is rather low.

In order to assist in choosing appropriate values of the parameter α, Table 4 lists the important characteristics of the Kaiser windows for different values of α. We discuss here in detail and show in the Appendix F the three cases $\alpha = 3$, $\alpha = 4$ and $\alpha = 5$:

Kaiser window with $\alpha = 3$: The transfer function and characteristics are shown in Figure 28 and are given by

$$\text{NENBW} = 1.7952\,\text{bins}\,, \tag{113}$$

$$W_{3\,\text{dB}} = 1.7025\,\text{bins}\,, \tag{114}$$

$$e_{\max} = -1.0226\,\text{dB} = -11.1069\,\%. \tag{115}$$

The first zero is located at $f = \pm 3.16$ bins. The highest sidelobe is -69.6 dB, located at $f = \pm 3.32$ bins. At the optimal overlap of 61.9%, the amplitude flatness is 0.938, the power flatness is 0.722, and the overlap correlation is 0.230 .

Kaiser window with $\alpha = 4$: The transfer function and characteristics are shown in Figure 29

and are given by

$$\text{NENBW} = 2.0533\,\text{bins}\,, \tag{116}$$
$$W_{3\,\text{dB}} = 1.9417\,\text{bins}\,, \tag{117}$$
$$e_{\max} = -0.7877\,\text{dB} = -8.6697\,\%. \tag{118}$$

The first zero is located at $f = \pm 4.12$ bins. The highest sidelobe is $-94.4\,\text{dB}$, located at $f = \pm 4.25$ bins. At the optimal overlap of 67.0%, the amplitude flatness is 0.925, the power flatness is 0.719, and the overlap correlation is 0.237 .

Kaiser window with $\alpha = 5$: The transfer function and characteristics are shown in Figure 30 and are given by

$$\text{NENBW} = 2.2830\,\text{bins}\,, \tag{119}$$
$$W_{3\,\text{dB}} = 2.1553\,\text{bins}\,, \tag{120}$$
$$e_{\max} = -0.6403\,\text{dB} = -7.1061\,\%. \tag{121}$$

The first zero is located at $f = \pm 5.10$ bins. The highest sidelobe is $-119.8\,\text{dB}$, located at $f = \pm 5.20$ bins. At the optimal overlap of 70.5%, the amplitude flatness is 0.919, the power flatness is 0.717, and the overlap correlation is 0.241 .

The Kaiser window is comparable in performance and potential applications to the Blackman-Harris and Nuttall windows discussed in the previous subsections. Due to its 'tunability' with the parameter α it can easily be optimized for a certain application. A small disadvantage might be the necessity to compute the Bessel function (112).

D Flat-Top windows

If one required result of the data processing is to determine the exact amplitude of a sinusoidal component in the input signal (as will be necessary for detector calibration purposes in GEO 600), all the windows discussed so far are rather unsatisfactory. The amplitude of the peak may be misestimated by 1 dB or more, depending on the precise location of the peak frequency within the closest frequency bin. The maximum amplitude error (as defined in Section 8.2) has been given as $e_{\max}$ in the descriptions above. For the best window so far in this respect, the 'Nuttall4' window, it is 0.62 dB corresponding to an amplitude error of about 7 %, too much for many purposes.

Hence some people, including the manufacturers of commercial spectrum analyzers, have developed window functions that are as flat as possible in the frequency domain for frequency offsets $-0.5 \le f \le 0.5$ (measured in frequency bins). These are known as 'flat-top windows'. The author is aware of only one paper, [Salvatore88], that gives formulae for flat-top windows. The windows from this paper are discussed in Section D.1.

Three more flat-top window functions that were found in various sources, such as user manuals from spectrum analyzers etc., are discussed in Section D.2.

Since none of these have a sidelobe rejection sufficient for the purposes of the GEO 600 data analysis, the author has developed several new flat-top windows, described in Section D.3 below.

All flat-top windows are defined in a manner similar to the Blackman-Harris window, i.e. as sum of a few cosine terms. All of them are *negative* in a fraction of their time-series representation.

Note also that these windows are not at all flat in the time domain (see graphs in Appendix F below).

All these flat-top windows have bandwidths of about 3...5 bins, roughly twice as wide as non-flat-top windows with comparable sidelobe suppression. In many situations this is not a severe disadvantage, because it can be compensated by choosing a smaller frequency resolution f_{res}, i.e. a larger value of the FFT length N, provided the the input data stream is long enough.

D.1 Published flat-top windows

The only paper known to the author that gives formulae of flat-top windows introduces 6 different flat-top windows (Reference [Salvatore88]).

These windows are defined as a weighted sum of cosine terms (as are the Hanning, Hamming, Blackman-Harris and Nuttall windows):

$$z = \frac{2\pi \cdot j}{N}, \quad j = 0 \ldots N-1, \tag{122}$$

$$w_j = \sum_{k=0}^{m} c_k \cos(k \cdot z) = c_0 + \sum_{k=1}^{m} c_k \cos(k \cdot z). \tag{123}$$

In a manner similar to Nuttall (see Section C.7) two different window functions are defined for each (fixed) number of cosine terms by requiring different conditions that translate into equations for the unknown coefficients of the cosine terms. In addition to the differentiability conditions (86), (87) and (88), one more condition is imposed on each of the window functions below:

$$a(f_k) = 0 \quad \text{for a certain} \quad f_k \lessapprox 0.5, \quad \text{i.e.} \quad f_k \approx 0.45. \tag{124}$$

This condition demands that the transfer function reaches a zero at a predefined frequency offset near the end of the $-0.5 \le f \le 0.5$ interval, thus making the transfer function nearly flat in that interval. The two types of window function for each number of terms are:

'fast decaying' (abbreviated 'F') that enforces the highest possible degree of differentiability at the boundary and thus the fastest possible sidelobe drop rate by requiring as many of the conditions (86), (87) and (88) as possible;

'minimum sidelobe' (abbreviated 'M') that uses the available degrees of freedom to minimize the level of the highest sidelobe. Actually in [Salvatore88] an analytical condition is used that enforces a zero of the transfer function at an arbitrarily selected frequency. This is not exactly equivalent to minimizing the level of the highest sidelobe, see also Section D.3.

The coefficients of the 6 window functions are summarized in Table 5. More information about each window can be found in Table 2 on page 29 and in the graph for each window, printed at the end of this report between pages 67 and 72. Note that there are some small discrepancies concerning the numbers given for the peak sidelobe level PSLL between the original paper[Salvatore88] and this work; the author believes that the numbers printed in this work are correct.

Name	c_0	c_1	c_2	c_3	c_4	SLDR f^{-n}	PSLL [dB]	Graph page
SFT3F	0.26526	−0.5	0.23474	0	0	3	−31.7	67
SFT4F	0.21706	−0.42103	0.28294	−0.07897	0	5	−44.7	68
SFT5F	0.1881	−0.36923	0.28702	−0.13077	0.02488	7	−57.3	69
SFT3M	0.28235	−0.52105	0.19659	0	0	1	−44.2	70
SFT4M	0.241906	−0.460841	0.255381	−0.041872	0	1	−66.5	71
SFT5M	0.209671	−0.407331	0.281225	−0.092669	0.0091036	1	−89.9	72

Table 5 *Coefficients of Salvatore flat-top window functions, to be used with Equation (123).*

D.1.1 Fast decaying 3-term flat top window

This window, called 'SFT3F' in this report, is derived by requiring the flatness condition (124) and a SLDR of f^{-3}. Its coefficients are taken from Ref. [Salvatore88] and listed in Table 5. The transfer function and characteristics are shown in Figure 31 on page 67 and are given by

$$\text{NENBW} = 3.1681\,\text{bins}\,, \tag{125}$$

$$W_{3\,\text{dB}} = 3.1502\,\text{bins}\,, \tag{126}$$

$$e_{\max} = 0.0082\,\text{dB} = 0.0946\,\%. \tag{127}$$

The first zero is located at $f = \pm 3.00$ bins. The highest sidelobe is $-31.7\,\text{dB}$, located at $f = \pm 3.37$ bins. At the optimal overlap of 66.7%, the amplitude flatness is 0.998, the power flatness is 0.558, and the overlap correlation is -0.029 .

D.1.2 Fast decaying 4-term flat top window

This window, called 'SFT4F' in this report, is derived by requiring the flatness condition (124) and a SLDR of f^{-5}. Its coefficients are taken from Ref. [Salvatore88] and listed in Table 5. The transfer function and characteristics are shown in Figure 32 on page 68 and are given by

$$\text{NENBW} = 3.7970\,\text{bins}\,, \tag{128}$$

$$W_{3\,\text{dB}} = 3.7618\,\text{bins}\,, \tag{129}$$

$$e_{\max} = 0.0041\,\text{dB} = 0.0472\,\%. \tag{130}$$

The first zero is located at $f = \pm 4.00$ bins. The highest sidelobe is $-44.7\,\text{dB}$, located at $f = \pm 4.33$ bins. At the optimal overlap of 75.0%, the amplitude flatness is 1.000, the power flatness is 0.647, and the overlap correlation is 0.039 .

D.1.3 Fast decaying 5-term flat top window

This window, called 'SFT5F' in this report, is derived by requiring the flatness condition (124) and a SLDR of f^{-7}. Its coefficients are taken from Ref. [Salvatore88] and listed in Table 5. The

transfer function and characteristics are shown in Figure 33 on page 69 and are given by

$$\text{NENBW} = 4.3412\,\text{bins}\,, \tag{131}$$

$$W_{3\,\text{dB}} = 4.2910\,\text{bins}\,, \tag{132}$$

$$e_{\max} = -0.0025\,\text{dB} = -0.0282\,\%. \tag{133}$$

The first zero is located at $f = \pm 5.00$ bins. The highest sidelobe is $-57.3\,\text{dB}$, located at $f = \pm 5.31$ bins. At the optimal overlap of 78.5%, the amplitude flatness is 0.969, the power flatness is 0.648, and the overlap correlation is 0.052 .

D.1.4 Minimum sidelobe 3-term flat top window

This window, called 'SFT3M' in this report, is derived by requiring the flatness condition (124) and using the remaining degree of freedom to reduce the peak sidelobe level. Its coefficients are taken from Ref. [Salvatore88] and listed in Table 5. The transfer function and characteristics are shown in Figure 34 on page 70 and are given by

$$\text{NENBW} = 2.9452\,\text{bins}\,, \tag{134}$$

$$W_{3\,\text{dB}} = 2.9183\,\text{bins}\,, \tag{135}$$

$$e_{\max} = -0.0115\,\text{dB} = -0.1323\,\%. \tag{136}$$

The first zero is located at $f = \pm 3.00$ bins. The highest sidelobe is $-44.2\,\text{dB}$, located at $f = \pm 5.50$ bins. The sidelobes drop at a rate of f^{-1}. At the optimal overlap of 65.5%, the amplitude flatness is 0.949, the power flatness is 0.584, and the overlap correlation is -0.005 .

D.1.5 Minimum sidelobe 4-term flat top window

This window, called 'SFT4M' in this report, is derived by requiring the flatness condition (124) and using the remaining two degrees of freedom to reduce the peak sidelobe level. Its coefficients are taken from Ref. [Salvatore88] and listed in Table 5. The transfer function and characteristics are shown in Figure 35 on page 71 and are given by

$$\text{NENBW} = 3.3868\,\text{bins}\,, \tag{137}$$

$$W_{3\,\text{dB}} = 3.3451\,\text{bins}\,, \tag{138}$$

$$e_{\max} = -0.0067\,\text{dB} = 0.0776\,\%. \tag{139}$$

The first zero is located at $f = \pm 4.00$ bins. The highest sidelobe is $-66.5\,\text{dB}$, located at $f = \pm 10.50$ bins. The sidelobes drop at a rate of f^{-1}. At the optimal overlap of 72.1%, the amplitude flatness is 0.964, the power flatness is 0.641, and the overlap correlation is 0.044 .

The HFT70 window (see Section D.3.1 on page 45) was designed with the same aims and reaches a better sidelobe suppression due to a better optimization procedure.

D.1.6 Minimum sidelobe 5-term flat top window

This window, called 'SFT5M' in this report, is derived by requiring the flatness condition (124) and using the remaining two degrees of freedom to reduce the peak sidelobe level.[9] Its coefficients

[9] In the original work [Salvatore88] it is claimed that the remaining degree of freedom was used to enforce condition (86) and thus ensure a SLDR of f^{-3}. The coefficients listed in the paper do not, however, exactly fulfill this condition and the sidelobes accordingly drop only as f^{-1} for $f > 300$, see Figure 36. The window HFT90D (see Section D.3.3 and Figure 42 on page 78) is very similar to SFT5M and exactly fulfills condition (86).

are taken from Ref. [Salvatore88] and listed in Table 5. The transfer function and characteristics are shown in Figure 35 on page 71 and are given by

$$\text{NENBW} = 3.8852\,\text{bins}\,, \tag{140}$$
$$W_{3\,\text{dB}} = 3.8340\,\text{bins}\,, \tag{141}$$
$$e_{\max} = 0.0039\,\text{dB} = 0.0449\,\%. \tag{142}$$

The first zero is located at $f = \pm 5.00$ bins. The highest sidelobe is $-89.9\,\text{dB}$, located at $f = \pm 5.12$ bins. The sidelobes drop at a rate of f^{-1}. At the optimal overlap of 76.0%, the amplitude flatness is 0.953, the power flatness is 0.645, and the overlap correlation is 0.053 .

D.2 Flat-top windows by instrument makers

Because of the practical importance of flat-top windows and the lack (until recently) of published information, the makers of spectrum analyzers and related software have developed their own flat-top windows. All those that the author could find in user manuals, web pages, usenet discussions etc. are discussed in this Section.

D.2.1 National Instruments flat-top window

This window function, abbreviated 'FTNI' in this report, is cited by National Instruments on its web page and is defined by

$$z = \frac{2\,\pi \cdot j}{N}, \quad j = 0 \ldots N-1, \tag{143}$$
$$w_j = 0.2810639 - 0.5208972\cos(z) + 0.1980399\cos(2z). \tag{144}$$

The transfer function and characteristics are shown in Figure 37 on page 73 and are given by

$$\text{NENBW} = 2.9656\,\text{bins}\,, \tag{145}$$
$$W_{3\,\text{dB}} = 2.9355\,\text{bins}\,, \tag{146}$$
$$e_{\max} = 0.0169\,\text{dB} = 0.1946\,\%. \tag{147}$$

The first zero is located at $f = \pm 3.00$ bins. The highest sidelobe is $-44.4\,\text{dB}$, located at $f = \pm 3.23$ bins. The sidelobes drop at a rate of f^{-1}. At the optimal overlap of 65.6%, the amplitude flatness is 0.950, the power flatness is 0.584, and the overlap correlation is -0.007 . This window is very similar to SFT3M (see Section D.1.4 and Figure 34 on page 70).

D.2.2 Old HP flat-top window

This window function, abbreviated 'FTHP' in this report, had been used in some older HP spectrum analyzers and is defined by

$$z = \frac{2\,\pi \cdot j}{N}, \quad j = 0 \ldots N-1, \tag{148}$$
$$w_j = 1.0 - 1.912510941\cos(z) + 1.079173272\cos(2z) - 0.1832630879\cos(3z). \tag{149}$$

Its transfer function and characteristics are shown in Figure 38 on page 74 and are given by

$$\text{NENBW} = 3.4279\,\text{bins}\,, \tag{150}$$
$$W_{3\,\text{dB}} = 3.3846\,\text{bins}\,, \tag{151}$$
$$e_{\max} = 0.0096\,\text{dB} = 0.1103\,\%. \tag{152}$$

The first zero is located at $f = \pm 4.00$ bins. The highest sidelobe is $-70.4\,\text{dB}$, located at $f = \pm 4.65$ bins. The sidelobes drop at a rate of f^{-1}. At the optimal overlap of 72.3%, the amplitude flatness is 0.966, the power flatness is 0.640, and the overlap correlation is 0.041 .

The HFT70 window (see Section D.3.1) is very similar to the FTHP window, it reaches the same sidelobe level with a smaller amplitude error $e_{\max}$ and a marginally smaller bandwidth.

D.2.3 Undisclosed HP flat-top window

Newer spectrum analyzers from HP/Agilent (such as the 3562 and 35670A) use another flat-top window. Agilent insists that the precise definition is 'proprietary' and cannot be given out without a non-disclosure agreement, disclosing only that it is 'a basic cosine function with 4 terms'. It is, however, possible to measure the transfer function of the flat-top window and compare it with the known flat-top windows. It turns out that the closest match is the 'HFT95' window (see Section D.3.2 and Figure 41 on page 77). The comparison is shown in Figure 14.

It can be seen that the 35670A flat-top window is very close to the 'HFT95' window, which also has a similar equivalent noise bandwidth. That value could not be found in the documentation either, but can be deduced from the conversion factor between measurements in V and $\text{V}/\sqrt{\text{Hz}}$, as described in Section 9. The normalized equivalent noise bandwidth of the 35670A flat-top window, as programmed into its software, is

$$\text{NENBW} = 3.819\,\text{bins}\,, \tag{153}$$

compared with $\text{NENBW} = 3.811\,\text{bins}$ for the 'HFT95' window.

D.2.4 Stanford Research flat-top window

This window function, abbreviated 'FTSRS' in this report, is used in the Stanford Research SR785 spectrum analyzer and is defined by (according to the user manual):

$$z = \frac{2\,\pi \cdot j}{N}, \quad j = 0 \ldots N-1, \tag{154}$$
$$w_j = 1.0 - 1.93\cos(z) + 1.29\cos(2z) - 0.388\cos(3z) + 0.028\cos(4z). \tag{155}$$

Its transfer function and characteristics are shown in Figure 39 on page 75 and are given by

$$\text{NENBW} = 3.7702\,\text{bins}\,, \tag{156}$$
$$W_{3\,\text{dB}} = 3.7274\,\text{bins}\,, \tag{157}$$
$$e_{\max} = -0.0156\,\text{dB} = -0.1796\,\%. \tag{158}$$

The first zero is located at $f = \pm 4.72$ bins. The highest sidelobe is $-76.6\,\text{dB}$, located at $f = \pm 5.37$ bins. The sidelobes drop at a rate of f^{-3}. At the optimal overlap of 75.4%, the amplitude flatness is 0.958, the power flatness is 0.647, and the overlap correlation is 0.055 .

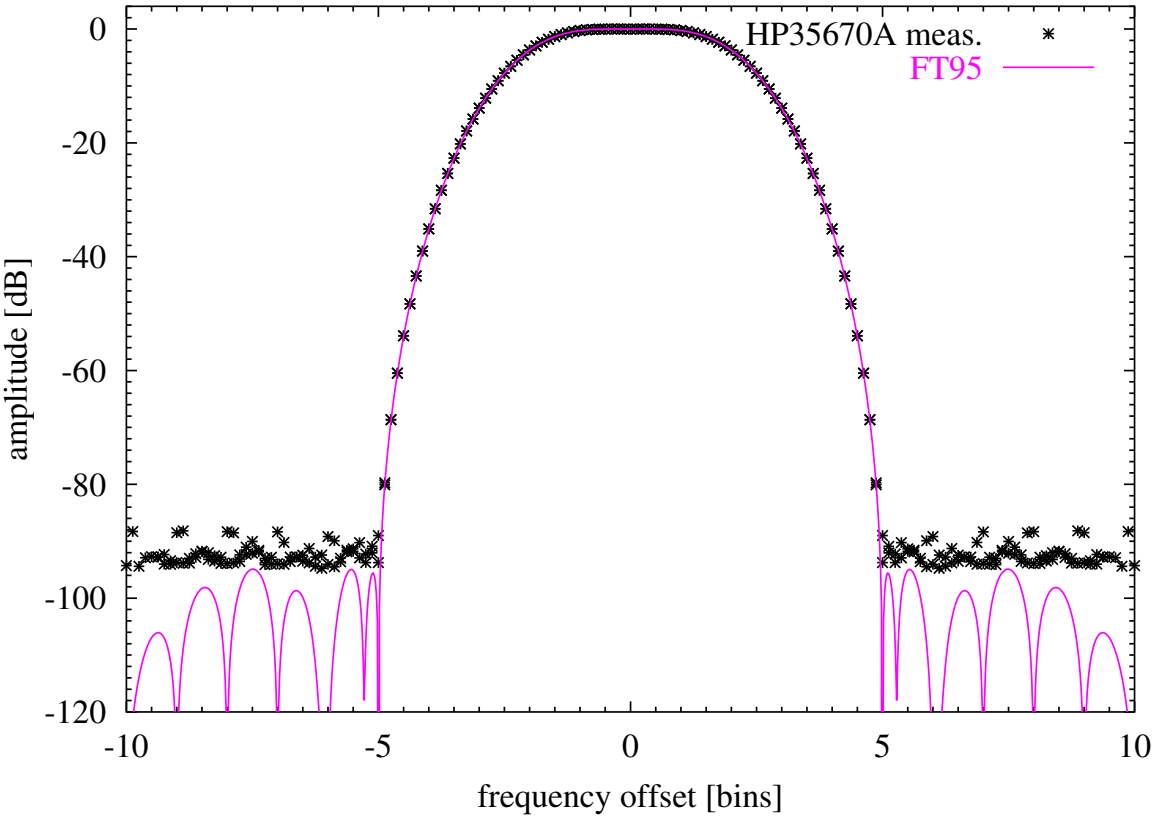

Figure 14 *Measured flat-top window of Agilent 35670A dynamic signal analyzer. The black asterisks represent the measured data, while the solid curve show the computed transfer function of the 'HFT95' flat-top window discussed in the text. The analyzer was set to a resolution of 1600 lines. For frequency offsets more than approximately* ± 5 *bins the measurement was dominated by the analyzer noise floor, which was approximately* $-93\,dB$ *in this measurement.*

D.3 New flat-top windows

Since the flat-top windows available so far are not sufficient for the the data analysis of GEO 600 in all situations,[10] new flat-top windows with improved characteristics have been developed by the author. Their basic form is again a sum of cosine terms, with the first term c_0 arbitrarily set to unity:[11]

$$z = \frac{2\pi \cdot j}{N}, \quad j = 0 \ldots N-1, \tag{159}$$

$$w_j = 1 + \sum_{k=1}^{m} c_k \cos(k \cdot z). \tag{160}$$

Most of the functions presented below additionally fulfill the condition

$$1 + \sum_{k=1}^{m} c_k = 0 \tag{161}$$

which ensures that the function is continuous at the boundary but at the same time implies that is also differentiable once and hence has a sidelobe dropping rate (SLDR) of f^{-3}. These functions are called 'HFTxx**D**' in this report, where the '**D**' stands for 'differentiable' and xx is the maximal sidelobe level in dB.[12] Those functions that do not fulfill Equation (161) are discontinuous at the boundary, have a SLDR of f^{-1} only and are called 'HFTxx'

The functions were developed by applying nonlinear optimization algorithms to a 'figure-of-merit' function that was formed as a combination of the flatness for $-0.5 \leq f \leq 0.5$, the width of the main lobe, and the peak sidelobe level. The parameters to be varied by the algorithms were the coefficients c_k of Equation (160). Up to 8 parameters were used in the optimization. The resulting window functions are presented below, with a short text section giving their formula and describing their main characteristics, and a detailed graph near the end of this report.

D.3.1 HFT70

This window was optimized for the lowest sidelobe level that is achieveable with 3 cosine terms, i.e. the same aims as were used for the SFT4M window (see Section D.1.5). Because of the better optimization procedure, a sidelobe level of $-70.4\,\mathrm{dB}$ was reached instead of $-66.5\,\mathrm{dB}$ in the case of the SFT4M window. The window is defined as (see also Equation (160)):

$$w_j = 1 - 1.90796\,\cos(z) + 1.07349\,\cos(2\,z) - 0.18199\,\cos(3\,z). \tag{162}$$

Its transfer function and characteristics are shown in Figure 40 on page 76 and are given by

$$\mathrm{NENBW} = 3.4129\,\mathrm{bins}\,, \tag{163}$$

$$W_{3\,\mathrm{dB}} = 3.3720\,\mathrm{bins}\,, \tag{164}$$

$$e_{\max} = -0.0065\,\mathrm{dB} = 0.0750\,\%. \tag{165}$$

[10] The dynamic range of signals digitized with the main data acquisition system, for example, can reach more than 120 dB, while the best flat-top window known so far has a sidelobe level of 90 dB only.

[11] The window can be defined with an arbitrary factor due to our use of the 'window sums' S_1 and S_2 in the normalization of the results (see Equations (23) and (24)). Setting the first term c_0 to unity simplified the optimization procedure that was used to find the coefficients c_k. Another possible normalization is the one chosen by Nuttall (see the footnote in SectionC.7)

[12] The 'H' can stand for 'high dynamic range', 'high sidelobe suppression' etc.

The first zero is located at $f = \pm 4.00$ bins. The highest sidelobe is $-70.4\,\mathrm{dB}$, located at $f = \pm 4.65$ bins. The sidelobes drop at a rate of f^{-1}. At the optimal overlap of 72.2%, the amplitude flatness is 0.964, the power flatness is 0.637, and the overlap correlation is 0.041 .

D.3.2 HFT95

This window was optimized for the lowest sidelobe level that is achieveable with 4 cosine terms. Its characteristics are very similar to those of the flat-top window that is used in newer HP/Agilent spectrum analyzers, see Section D.2.3. The window is defined as (see also Equation (160)):

$$\begin{aligned} w_j = 1 &- 1.9383379\,\cos(z) + 1.3045202\,\cos(2\,z) \\ &- 0.4028270\,\cos(3\,z) + 0.0350665\,\cos(4\,z). \end{aligned} \tag{166}$$

Its transfer function and characteristics are shown in Figure 41 on page 77 and are given by

$$\mathrm{NENBW} = 3.8112\,\mathrm{bins}\,, \tag{167}$$

$$W_{3\,\mathrm{dB}} = 3.7590\,\mathrm{bins}\,, \tag{168}$$

$$e_{\max} = 0.0044\,\mathrm{dB} = 0.0507\,\%. \tag{169}$$

The first zero is located at $f = \pm 5.00$ bins. The highest sidelobe is $-95.0\,\mathrm{dB}$, located at $f = \pm 7.49$ bins. The sidelobes drop at a rate of f^{-1}. At the optimal overlap of 75.6%, the amplitude flatness is 0.952, the power flatness is 0.647, and the overlap correlation is 0.056 .

D.3.3 HFT90D

This window was optimized for the lowest sidelobe level that is achieveable with 4 cosine terms if condition (161) is additionally imposed to ensure a sidelobe-drop rate of f^{-3}. It is very similar to the SFT5M window (see Section D.1.6), although HFT90D achieves the same sidelobe level at a marginally smaller bandwidth and with a sidelobe drop rate of f^{-3} instead of f^{-1}. The window is defined as (see also Equation (160)):

$$\begin{aligned} w_j = 1 &- 1.942604\,\cos(z) + 1.340318\,\cos(2\,z) \\ &- 0.440811\,\cos(3\,z) + 0.043097\,\cos(4\,z). \end{aligned} \tag{170}$$

Its transfer function and characteristics are shown in Figure 42 on page 78 and are given by

$$\mathrm{NENBW} = 3.8832\,\mathrm{bins}\,, \tag{171}$$

$$W_{3\,\mathrm{dB}} = 3.8320\,\mathrm{bins}\,, \tag{172}$$

$$e_{\max} = -0.0039\,\mathrm{dB} = 0.0450\,\%. \tag{173}$$

The first zero is located at $f = \pm 5.00$ bins. The highest sidelobe is $-90.2\,\mathrm{dB}$, located at $f = \pm 5.58$ bins. The sidelobes drop at a rate of f^{-3}. At the optimal overlap of 76.0%, the amplitude flatness is 0.953, the power flatness is 0.646, and the overlap correlation is 0.054 .

D.3.4 HFT116D

This window was optimized for the lowest sidelobe level that is achieveable with 5 cosine terms if condition (161) is additionally imposed to ensure a sidelobe-drop rate of f^{-3}. The window is defined as (see also Equation (160)):

$$\begin{aligned} w_j = 1 &- 1.9575375\,\cos(z) + 1.4780705\,\cos(2\,z) - 0.6367431\,\cos(3\,z) \\ &+ 0.1228389\,\cos(4\,z) - 0.0066288\,\cos(5\,z). \end{aligned} \tag{174}$$

Its transfer function and characteristics are shown in Figure 43 on page 79 and are given by

$$\mathrm{NENBW} = 4.2186\,\mathrm{bins}\,, \tag{175}$$

$$W_{3\,\mathrm{dB}} = 4.1579\,\mathrm{bins}\,, \tag{176}$$

$$e_{\max} = -0.0028\,\mathrm{dB} = 0.0326\,\%. \tag{177}$$

The first zero is located at $f = \pm 6.00$ bins. The highest sidelobe is $-116.8\,\mathrm{dB}$, located at $f = \pm 7.52$ bins. At the optimal overlap of 78.2%, the amplitude flatness is 0.947, the power flatness is 0.651, and the overlap correlation is 0.063 .

D.3.5 HFT144D

This window was optimized for the lowest sidelobe level that is achieveable with 6 cosine terms if condition (161) is additionally imposed to ensure a sidelobe-drop rate of f^{-3}. The window is defined as (see also Equation (160)):

$$\begin{aligned} w_j = 1 &- 1.96760033\,\cos(z) + 1.57983607\,\cos(2\,z) - 0.81123644\,\cos(3\,z) \\ &+ 0.22583558\,\cos(4\,z) - 0.02773848\,\cos(5\,z) + 0.00090360\,\cos(6\,z). \end{aligned} \tag{178}$$

Its transfer function and characteristics are shown in Figure 44 on page 80 and are given by

$$\mathrm{NENBW} = 4.5386\,\mathrm{bins}\,, \tag{179}$$

$$W_{3\,\mathrm{dB}} = 4.4697\,\mathrm{bins}\,, \tag{180}$$

$$e_{\max} = 0.0021\,\mathrm{dB} = 0.0245\,\%. \tag{181}$$

The first zero is located at $f = \pm 7.00$ bins. The highest sidelobe is $-144.1\,\mathrm{dB}$, located at $f = \pm 7.07$ bins. At the optimal overlap of 79.9%, the amplitude flatness is 0.942, the power flatness is 0.655, and the overlap correlation is 0.069 .

D.3.6 HFT169D

This window was optimized for the lowest sidelobe level that is achieveable with 7 cosine terms if condition (161) is additionally imposed to ensure a sidelobe-drop rate of f^{-3}. The window is defined as (see also Equation (160)):

$$\begin{aligned} w_j = 1 &- 1.97441842\,\cos(z) + 1.65409888\,\cos(2\,z) - 0.95788186\,\cos(3\,z) \\ &+ 0.33673420\,\cos(4\,z) - 0.06364621\,\cos(5\,z) \\ &+ 0.00521942\,\cos(6\,z) - 0.00010599\,\cos(7\,z). \end{aligned} \tag{182}$$

Its transfer function and characteristics are shown in Figure 45 on page 81 and are given by

$$\begin{aligned} \text{NENBW} &= 4.8347\,\text{bins}\,, && (183)\\ W_{3\,\text{dB}} &= 4.7588\,\text{bins}\,, && (184)\\ e_{\max} &= 0.0017\,\text{dB} = 0.0191\,\%. && (185) \end{aligned}$$

The first zero is located at $f = \pm 8.00$ bins. The highest sidelobe is $-169.5\,\text{dB}$, located at $f = \pm 10.41$ bins. At the optimal overlap of 81.2%, the amplitude flatness is 0.938, the power flatness is 0.654, and the overlap correlation is 0.072 .

D.3.7 HFT196D

This window was optimized for the lowest sidelobe level that is achieveable with 8 cosine terms if condition (161) is additionally imposed to ensure a sidelobe-drop rate of f^{-3}. The window is defined as (see also Equation (160)):

$$\begin{aligned} w_j = 1 &- 1.979280420\,\cos(z) + 1.710288951\,\cos(2\,z) - 1.081629853\,\cos(3\,z)\\ &+ 0.448734314\,\cos(4\,z) - 0.112376628\,\cos(5\,z) + 0.015122992\,\cos(6\,z)\\ &- 0.000871252\,\cos(7\,z) + 0.000011896\,\cos(8\,z). \end{aligned} \quad (186)$$

Its transfer function and characteristics are shown in Figure 46 on page 82 and are given by

$$\begin{aligned} \text{NENBW} &= 5.1134\,\text{bins}\,, && (187)\\ W_{3\,\text{dB}} &= 5.0308\,\text{bins}\,, && (188)\\ e_{\max} &= 0.0013\,\text{dB} = 0.0153\,\%. && (189) \end{aligned}$$

The first zero is located at $f = \pm 9.00$ bins. The highest sidelobe is $-196.2\,\text{dB}$, located at $f = \pm 9.06$ bins. At the optimal overlap of 82.3%, the amplitude flatness is 0.936, the power flatness is 0.656, and the overlap correlation is 0.075 .

D.3.8 HFT223D

This window was optimized for the lowest sidelobe level that is achieveable with 9 cosine terms if condition (161) is additionally imposed to ensure a sidelobe-drop rate of f^{-3}. The window is defined as (see also Equation (160)):

$$\begin{aligned} w_j = 1 &- 1.98298997309\,\cos(z) + 1.75556083063\,\cos(2\,z)\\ &- 1.19037717712\,\cos(3\,z) + 0.56155440797\,\cos(4\,z)\\ &- 0.17296769663\,\cos(5\,z) + 0.03233247087\,\cos(6\,z)\\ &- 0.00324954578\,\cos(7\,z) + 0.00013801040\,\cos(8\,z)\\ &- 0.00000132725\,\cos(9\,z). \end{aligned} \quad (190)$$

Its transfer function and characteristics are shown in Figure 47 on page 83 and are given by

$$\begin{aligned} \text{NENBW} &= 5.3888\,\text{bins}\,, && (191)\\ W_{3\,\text{dB}} &= 5.3000\,\text{bins}\,, && (192)\\ e_{\max} &= -0.0011\,\text{dB} = -0.0129\,\%. && (193) \end{aligned}$$

The first zero is located at $f = \pm 10.00$ bins. The highest sidelobe is $-223.0\,\text{dB}$, located at $f = \pm 11.38$ bins. At the optimal overlap of 83.3%, the amplitude flatness is 0.936, the power flatness is 0.659, and the overlap correlation is 0.079 .

D.3.9 HFT248D

This window was optimized for the lowest sidelobe level that is achieveable with 10 cosine terms if condition (161) is additionally imposed to ensure a sidelobe-drop rate of f^{-3}. The window is defined as (see also Equation (160)):

$$\begin{aligned} w_j = 1 &- 1.985844164102\,\cos(z) + 1.791176438506\,\cos(2\,z) \\ &- 1.282075284005\,\cos(3\,z) + 0.667777530266\,\cos(4\,z) \\ &- 0.240160796576\,\cos(5\,z) + 0.056656381764\,\cos(6\,z) \\ &- 0.008134974479\,\cos(7\,z) + 0.000624544650\,\cos(8\,z) \\ &- 0.000019808998\,\cos(9\,z) + 0.000000132974\,\cos(10\,z). \end{aligned} \tag{194}$$

Its transfer function and characteristics are shown in Figure 48 on page 84 and are given by

$$\mathrm{NENBW} = 5.6512\,\mathrm{bins}\,, \tag{195}$$

$$W_{3\,\mathrm{dB}} = 5.5567\,\mathrm{bins}\,, \tag{196}$$

$$e_{\max} = 0.0009\,\mathrm{dB} = 0.0104\,\%. \tag{197}$$

The first zero is located at $f = \pm 11.00$ bins. The highest sidelobe is $-248.4\,\mathrm{dB}$, located at $f = \pm 13.37$ bins. At the optimal overlap of 84.1%, the amplitude flatness is 0.934, the power flatness is 0.659, and the overlap correlation is 0.080 .

E Bibliography and Acknowledgements

References

[FFTW] FFTW subroutine package, available under GPL from
`http://www.fftw.org/`

[Harris78] Fredric J. Harris: 'On the Use of Windows for Harmonic Analysis with the Discrete Fourier Transform', Proceedings of the IEEE, Vol. 66 (1): 51–83, Jan 1978

[Nuttall81] A.H. Nuttall: 'Some windows with very good sidelobe behaviour', IEEE Trans. on Acoustics, Speech and Signal Processing, Vol ASSP-29 (1): 84–91 (1981).

[Salvatore88] L. Salvatore, A. Trotta: 'Flat-top windows for PWM waveform processing via DFT', IEE proceedings, Vol. 135, Part B, (6) 346–361 (1988).

[Trethewey2000] M.W. Trethewey: 'Window and overlap processing effects on power estimates from spectra', Mech. Syst. and Signal Process., Vol. 14 (2) 267–278, 2000.

[Lyons] Richard G. Lyons: 'Understanding Digital Signal Processing', Addison-Wesley 1997.

[Press] W.H. Press, S.A. Teukolsky, W.T. Vetterling, B.P. Flannery: 'Numerical Recipes in C, The Art of Scientific Computing', Cambridge University Press, 2nd ed., 1992.

[Schutz] B.F. Schutz: 'Relation between Continuous and Discrete Fourier Transforms', internal note, April 1992.

[1] P.D. Welch: 'The Use of Fast Fourier Transform for the Estimation of Power Spectra: A Method Based on Time Averaging Over Short, Modified Periodograms,' IEEE Trans. Audio Electroacoustics, Vol. AU-15 (June 1967), 70-73.

Acknowlegdements

The authors wish to thank K. Kawabe, K. Kötter, A. Weidner and U. Weiland for their proof-reading of the manuscript and their various useful comments.

F Graphs of window functions

This appendix shows one comprehensive graph that includes the most important characteristics for each window function discussed in the text. The first plot for each window shows the window function in the time domain. For the plot it is normalized by computing

$$w'_j = w_j \frac{N}{S_1} \,. \tag{198}$$

Such a normalization is not necessary for the real application of the window, since we will use S_1 in the scaling of the results (see Section 9). In fact, we can compute the window values w_j with any convenient constant factor for this reason.

The next four plots show the transfer function of the window function in the frequency domain, with different x-axes. In the second of these plots the 3 dB bandwidth $W_{3\,\mathrm{dB}}$ is indicated with two small red arrows. The last of these plots has a logarithmic x-axis up to 10 000 bins in order to show the decay of the sidelobes far away from the main peak. For some of the window functions which have a very steep decay (see e.g. Figure 24 on page 60), the sidelobe level falls below -300 dB or so within the plot range and cannot be computed numerically any more; in these cases the last part of the curve shown is dominated by numerical noise. When comparing window functions, note that the y-axes are different for each window.

The last plot shows the overlap behaviour of the window, as discussed in Section 10. The vertical arrow is drawn at the position of the recommended overlap (ROV), as defined in that Section. For those windows that do not drop to zero at their end, again there is some numerical instability in the computation which shows up as non-smooth steps mainly in the 'amplitude flatness' curve (see also the discussion in Section C.5 on page 32 about the Hamming window, where this effect is most noticeable). For the flat-top windows, which are negative in a fraction of their time-domain representation, the amplitude flatness (AF) and overlap correlation (OC) also become negative for small values of the overlap.

All graphs and bandwidths below have been numerically computed with actual discrete window functions, using $N = 1000$, except for the 5th plot (logarithmic x-axis up to 10 000 bins), which uses $N = 30\,000$.

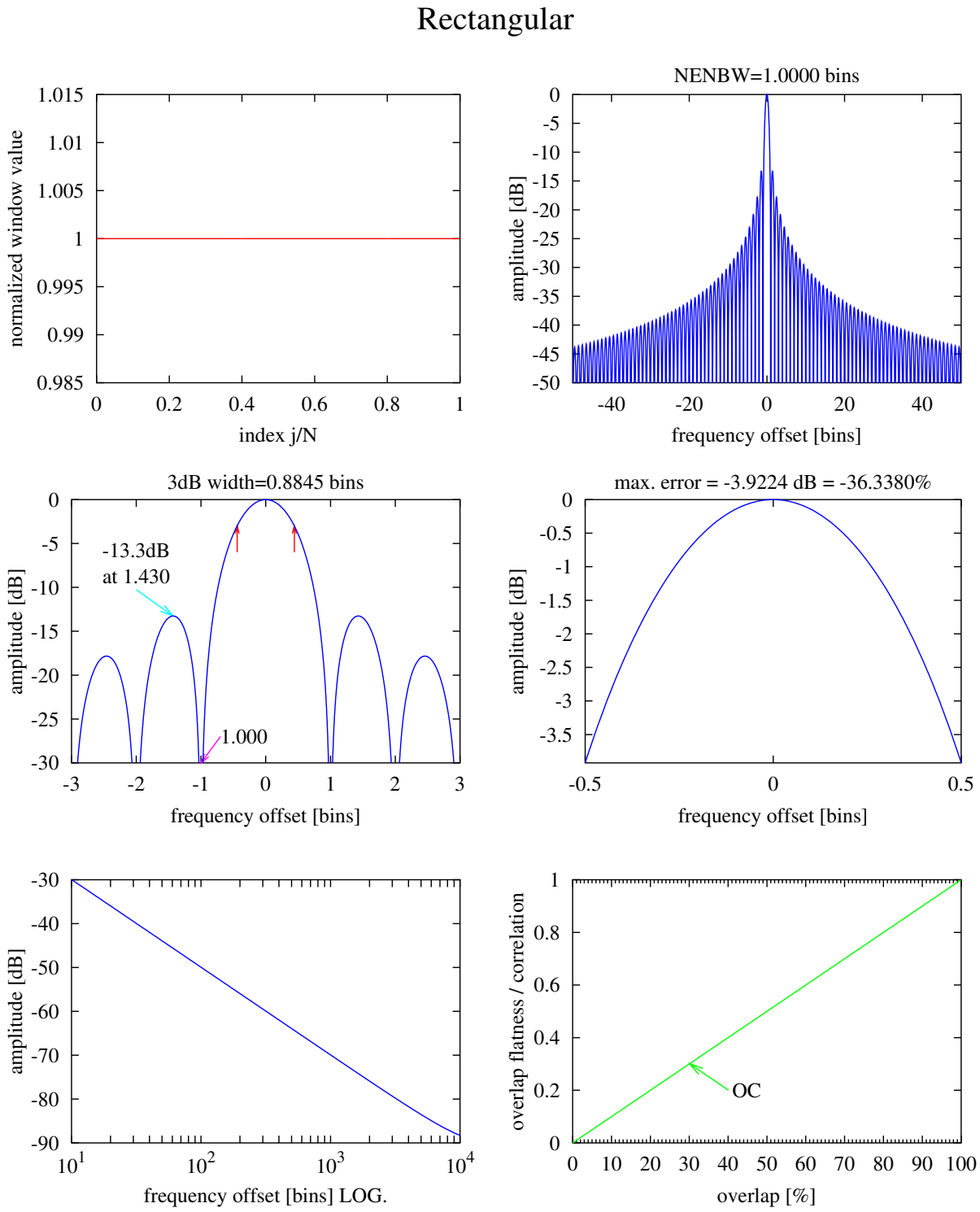

Figure 15 *Rectangular window. See text Section C.1 on page 30.*

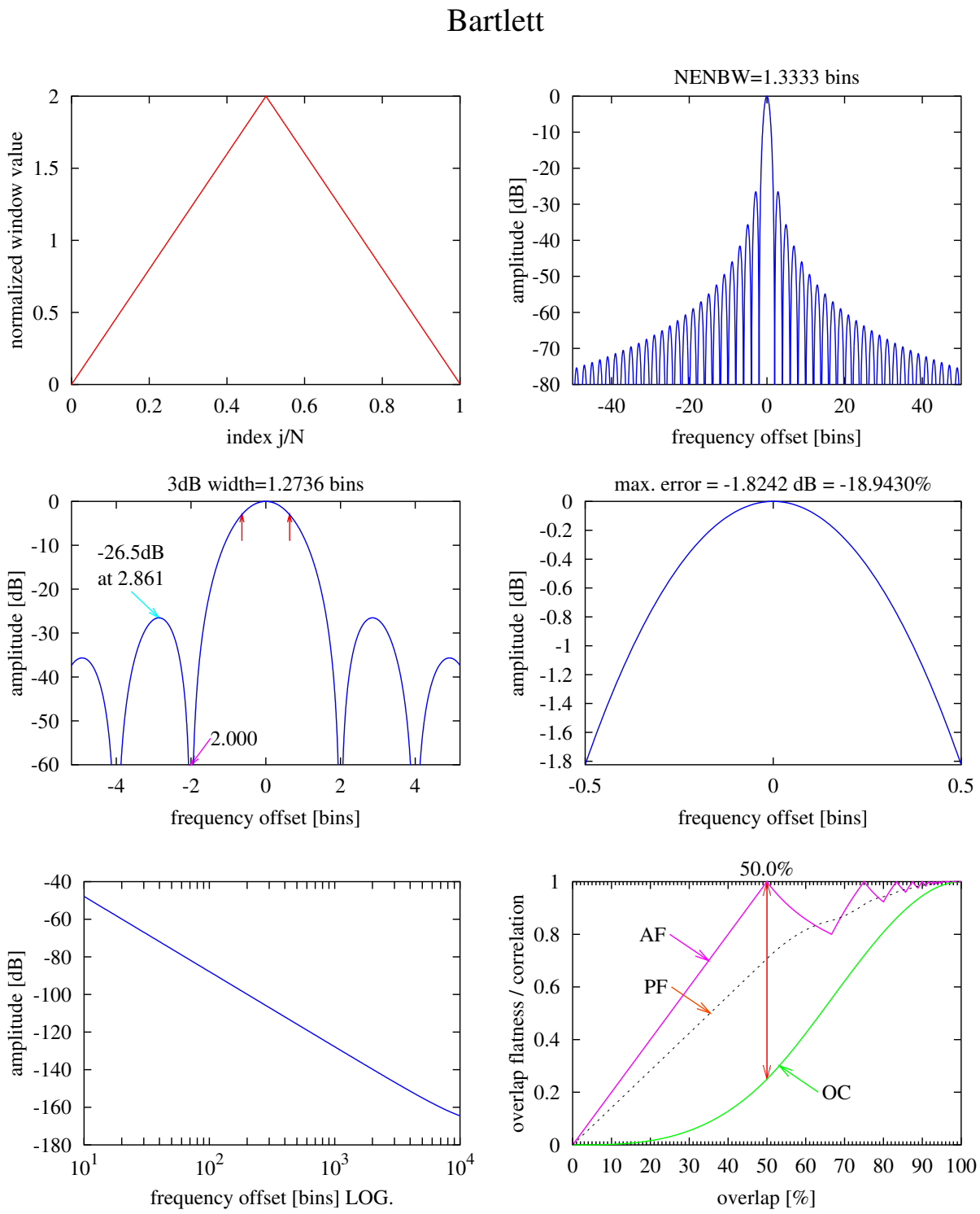

Figure 16 *Bartlett window. See text Section C.2 on page 30.*

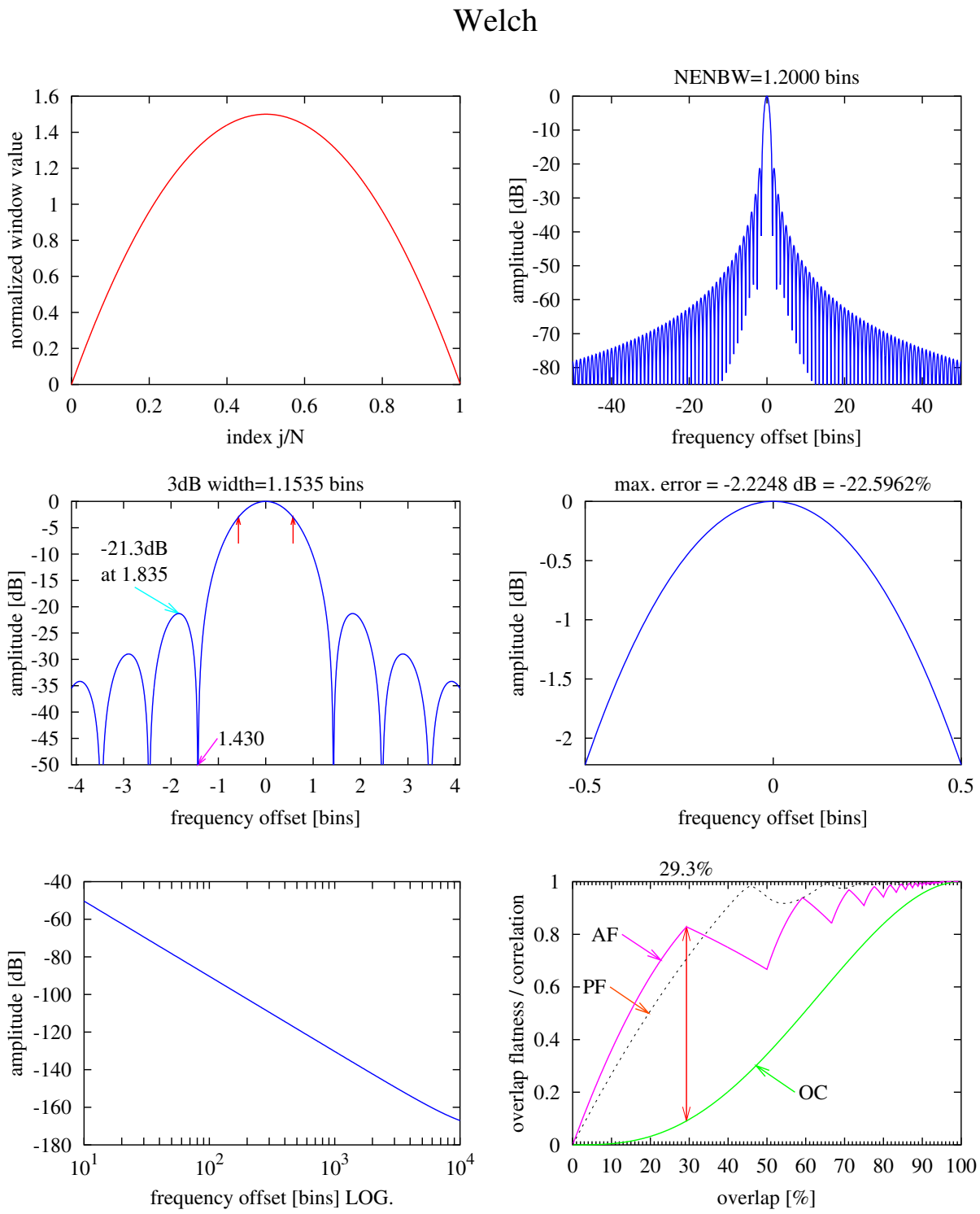

Figure 17 *Welch window. See text Section C.3 on page 31.*

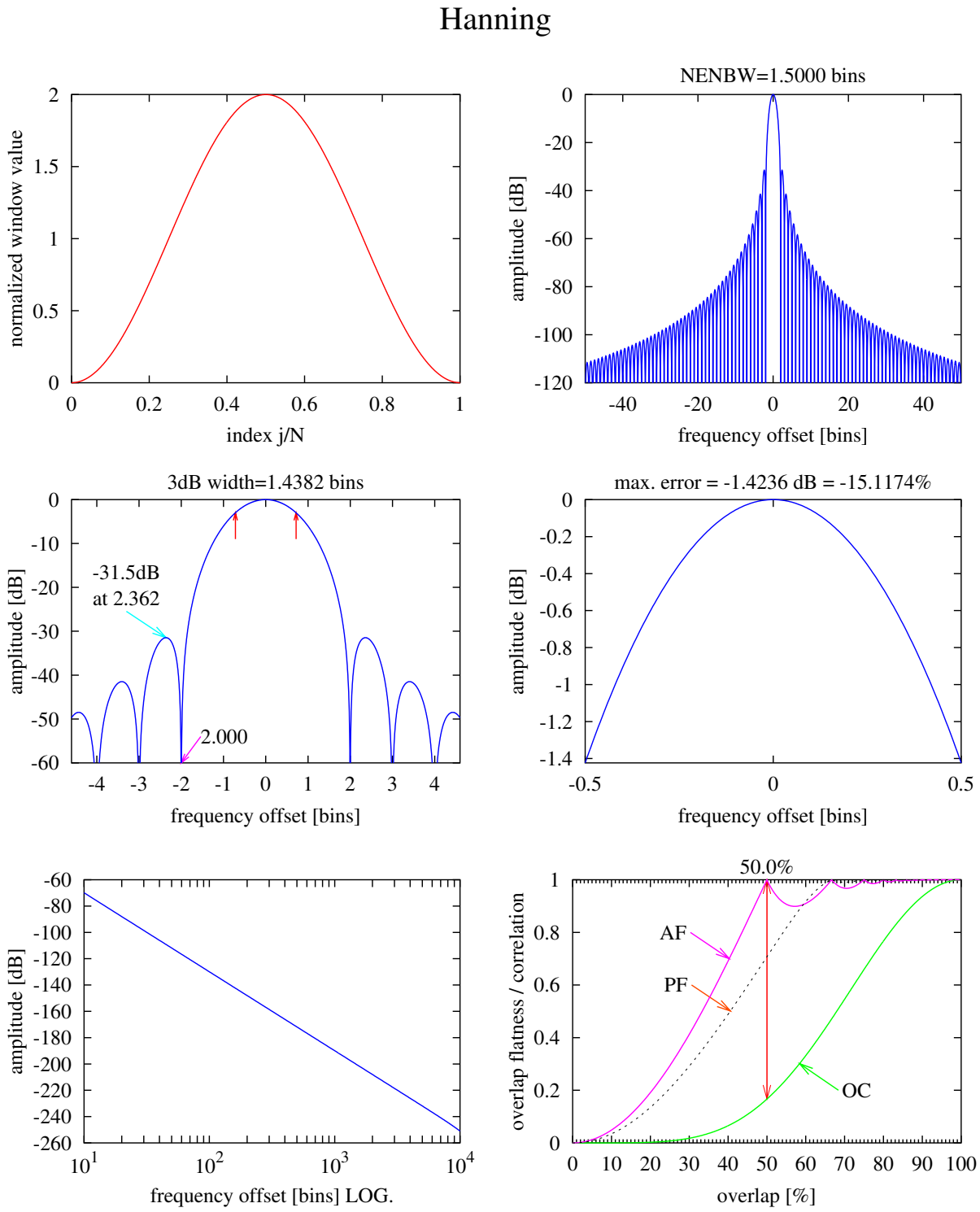

Figure 18 *Hanning window. See text Section C.4 on page 31.*

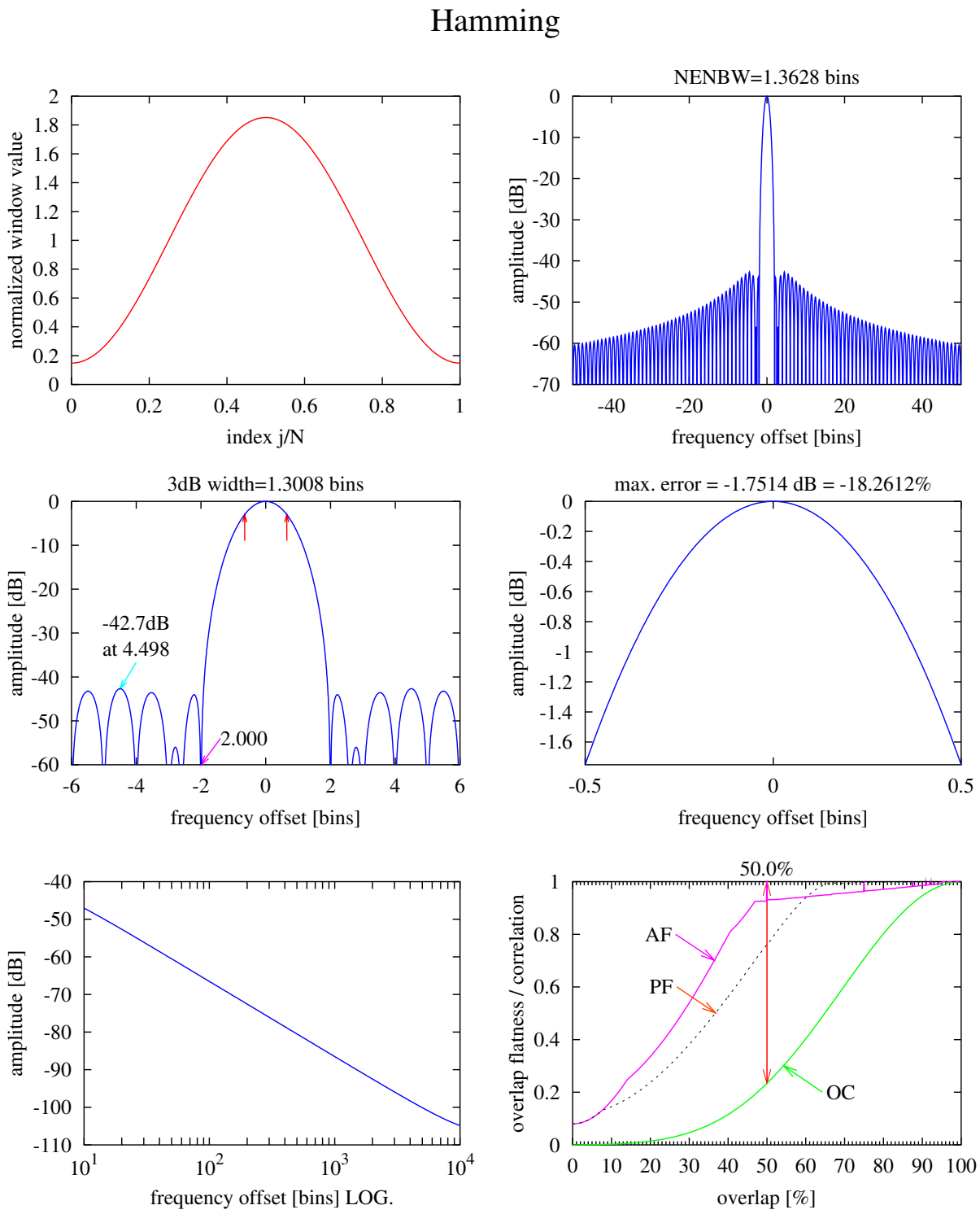

Figure 19 *Hamming window. See text Section C.5 on page 32.*

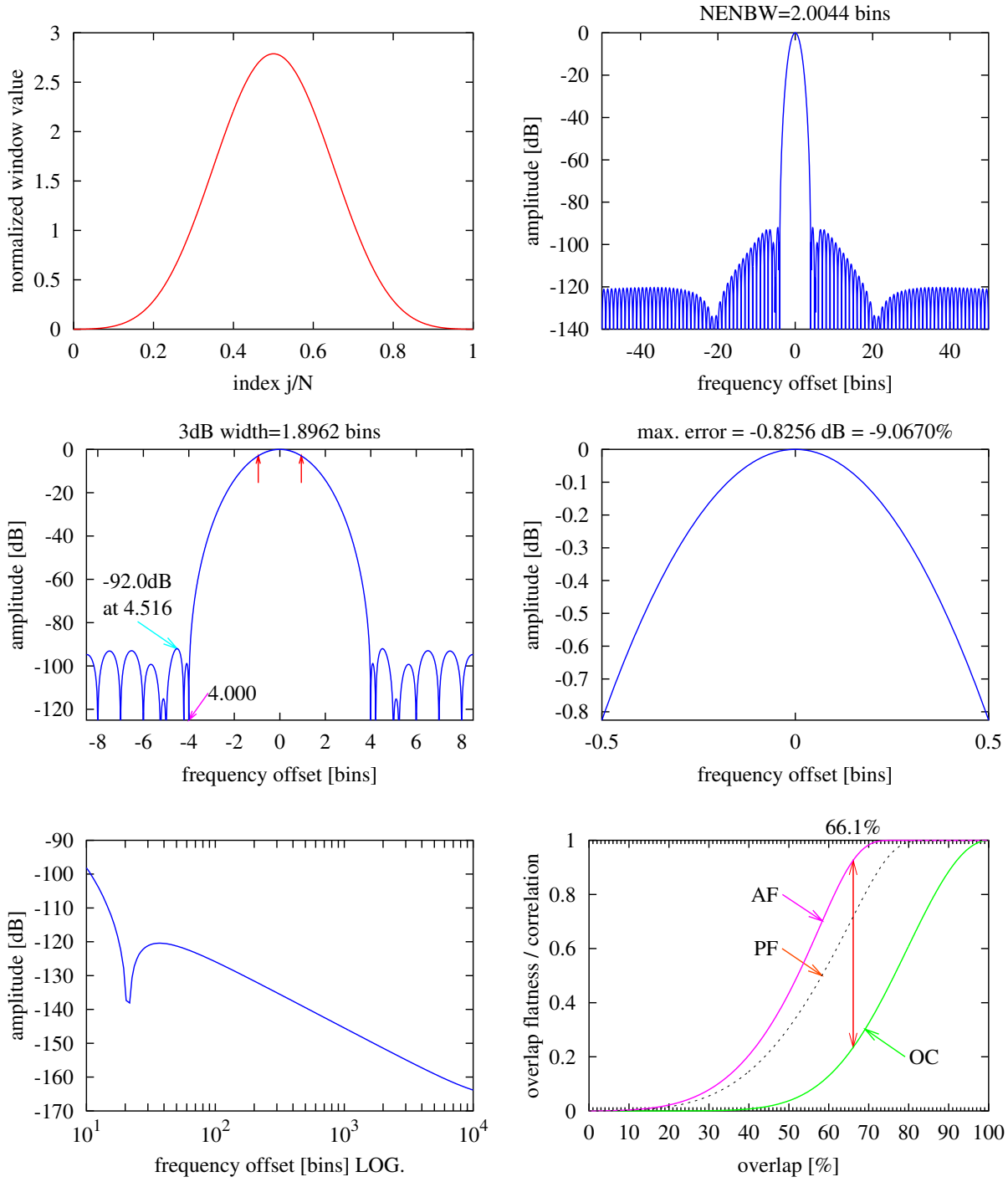

Figure 20 *92 dB Blackman-Harris window. See text Section C.6 on page 32.*

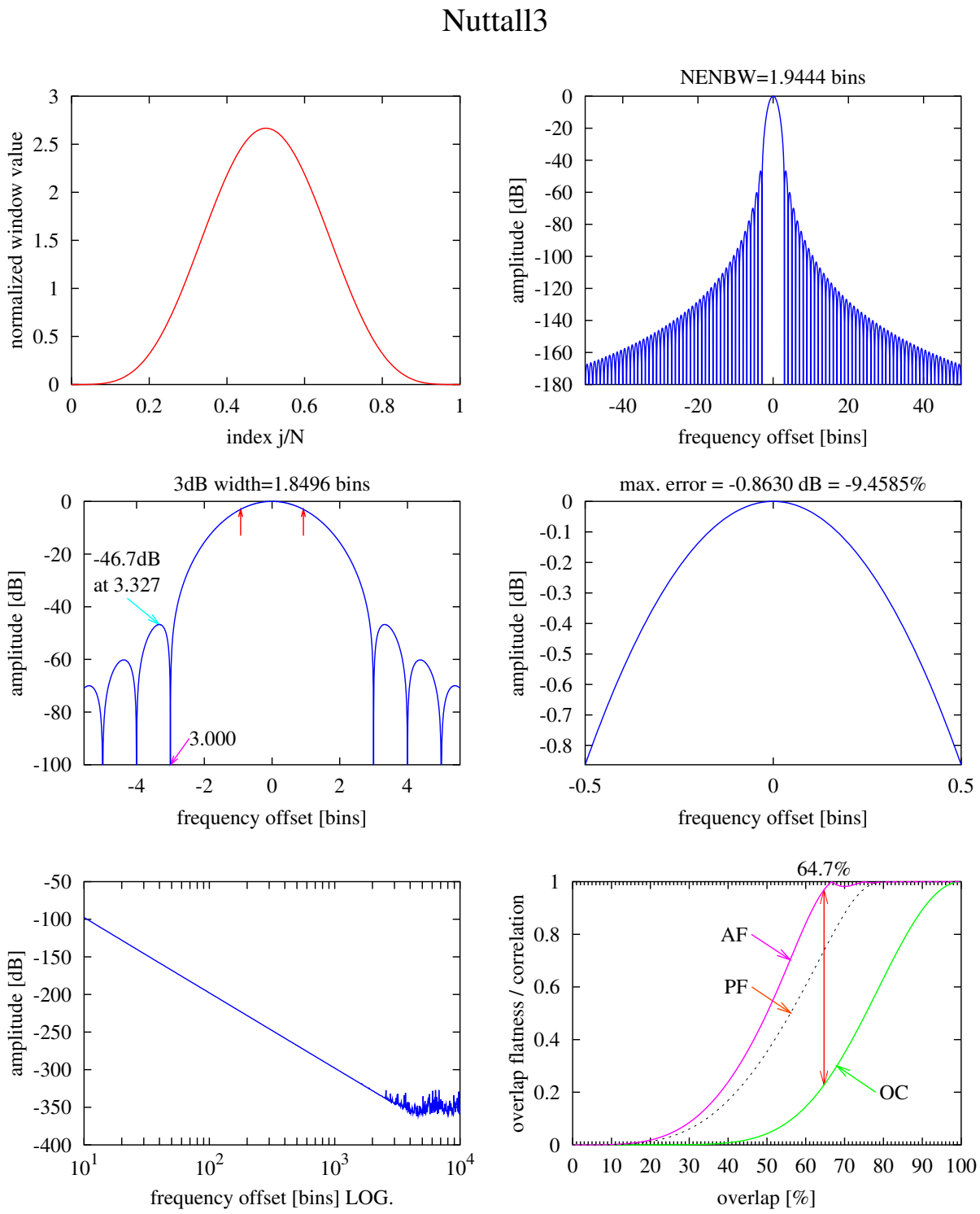

Figure 21 *Nuttall3 window. See text Section C.7.1 on page 34.*

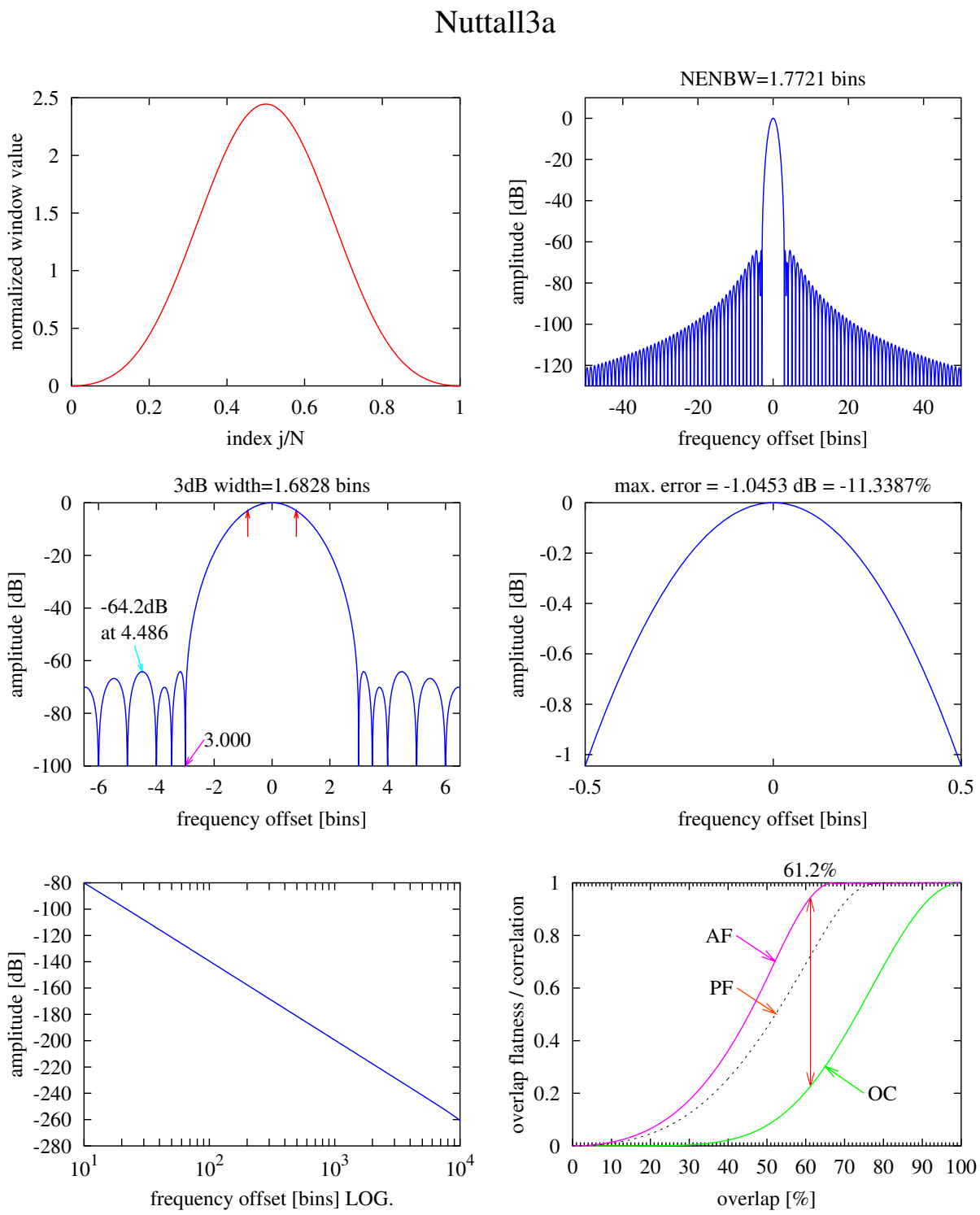

Figure 22 *Nuttall3a window. See text Section C.7.2 on page 35.*

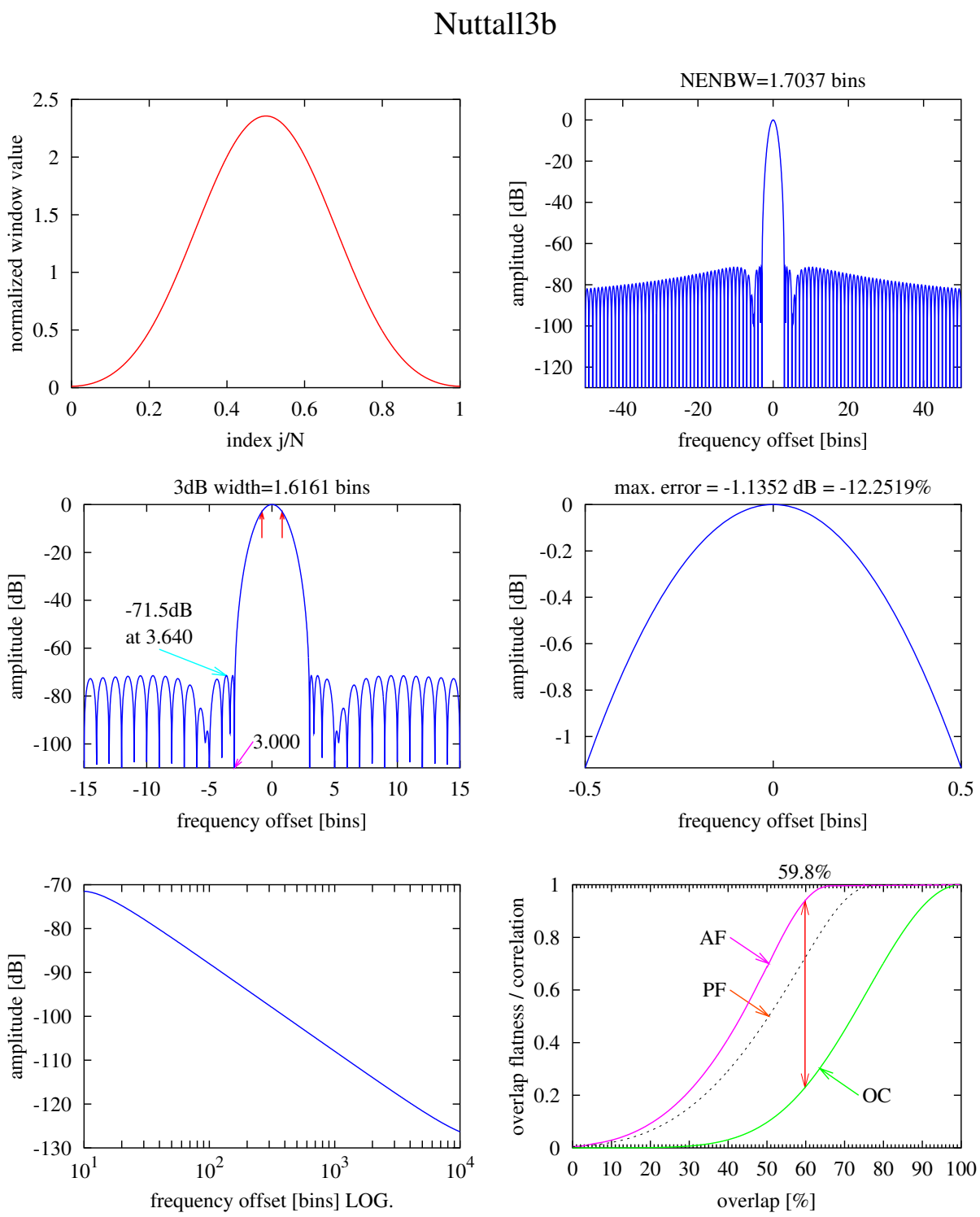

Figure 23 *Nuttall3b window. See text Section C.7.3 on page 35.*

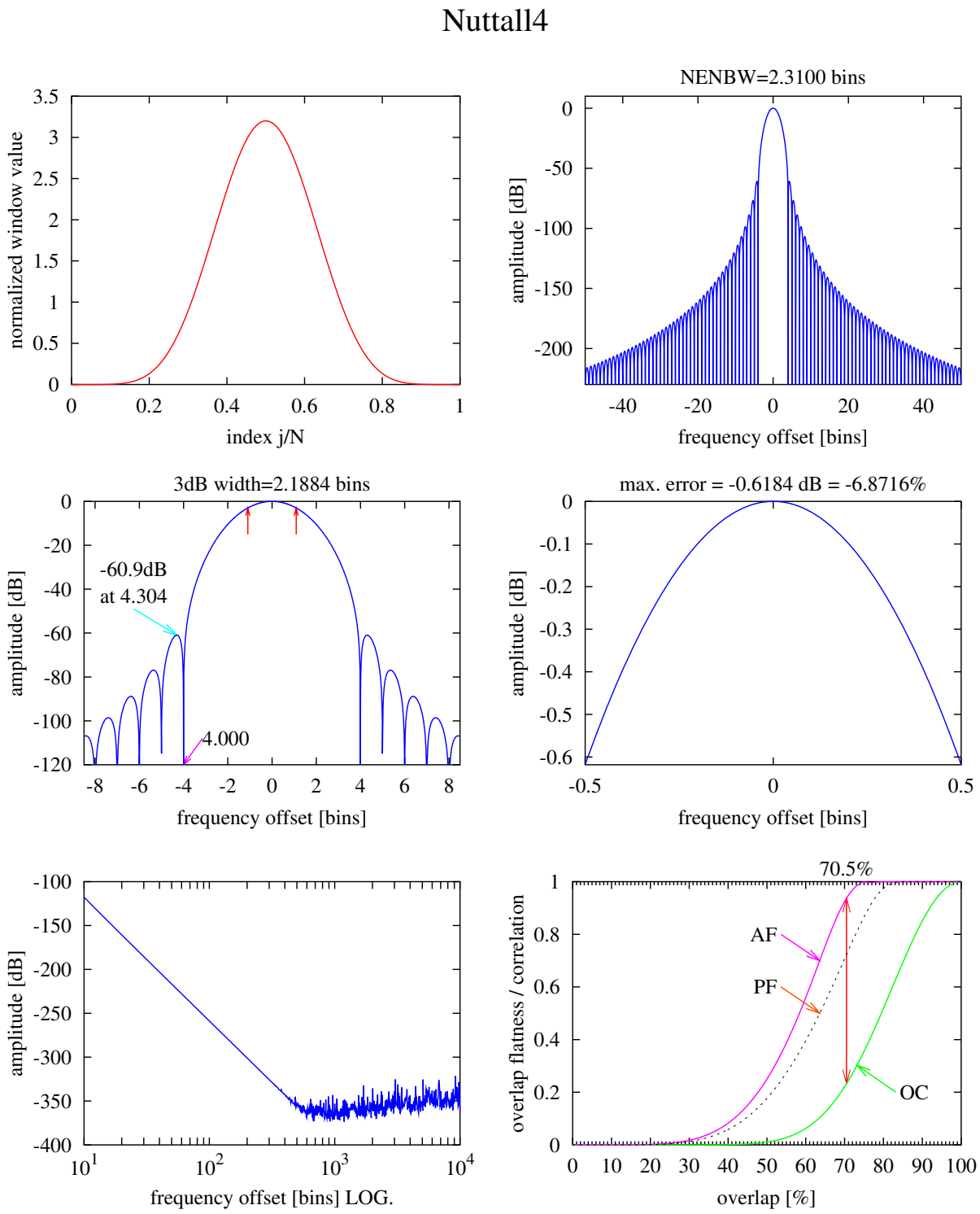

Figure 24 *Nuttall4 window. See text Section C.7.4 on page 35.*

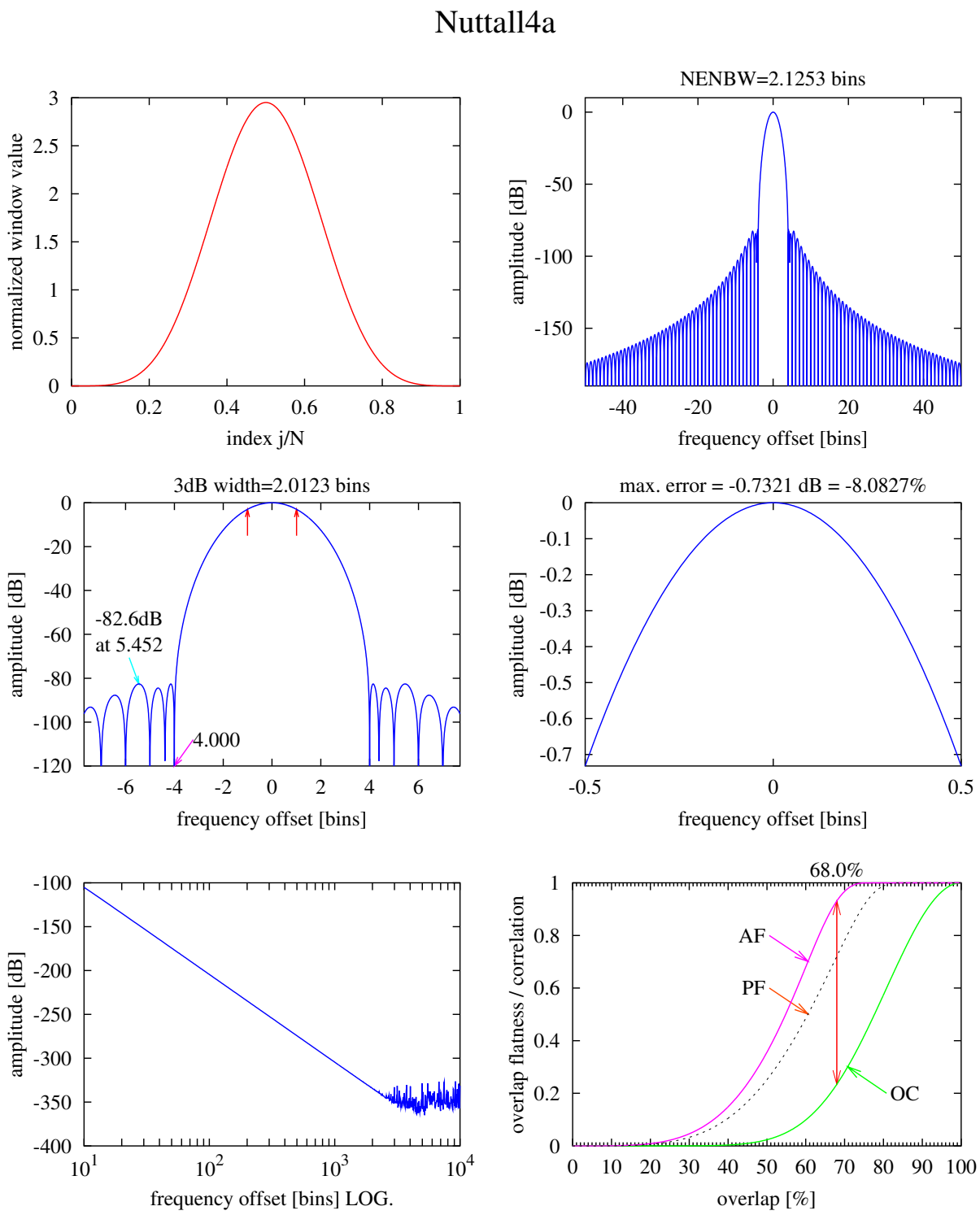

Figure 25 *Nuttall4a window. See text Section C.7.5 on page 35.*

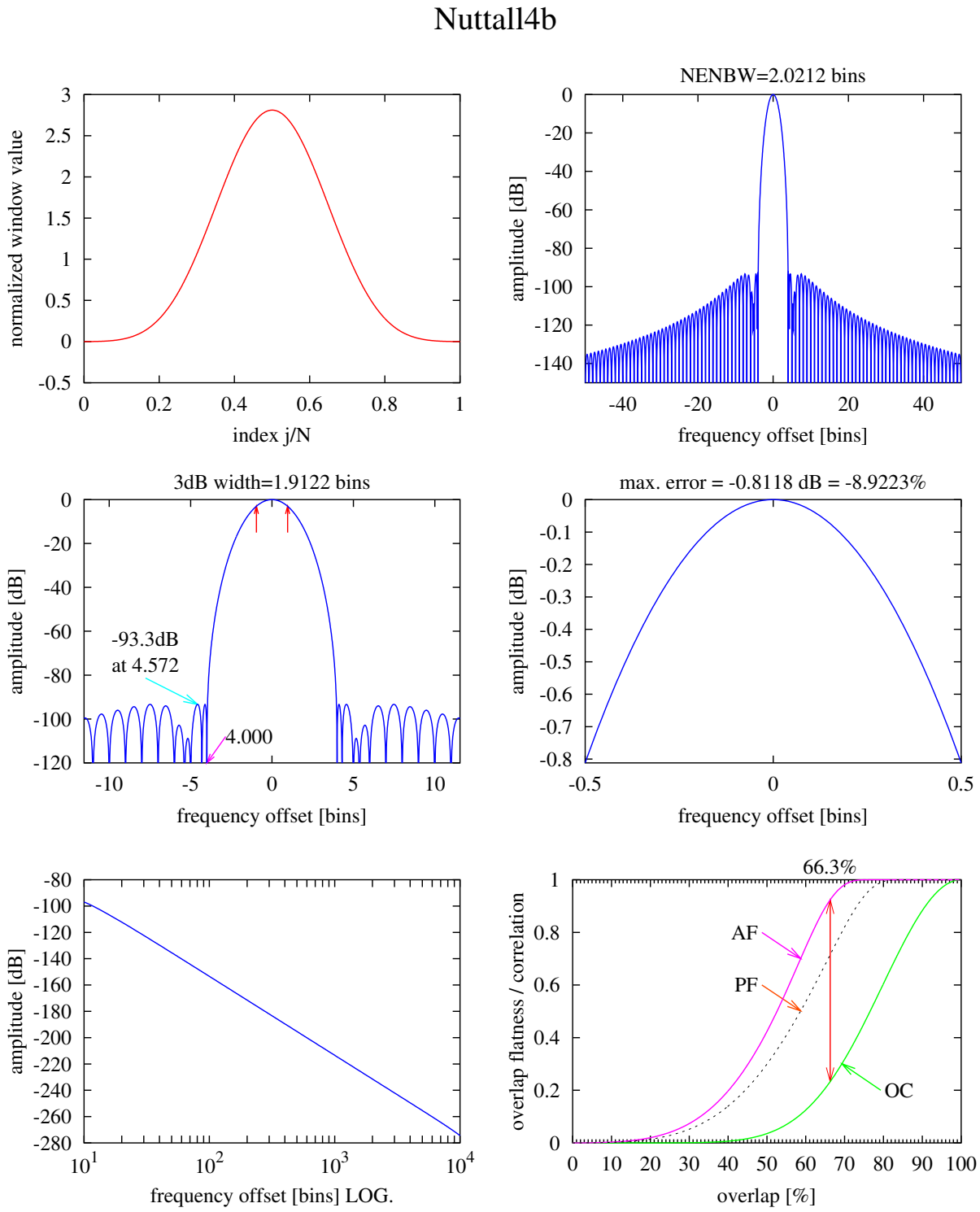

Figure 26 *Nuttall4b window. See text Section C.7.6 on page 36.*

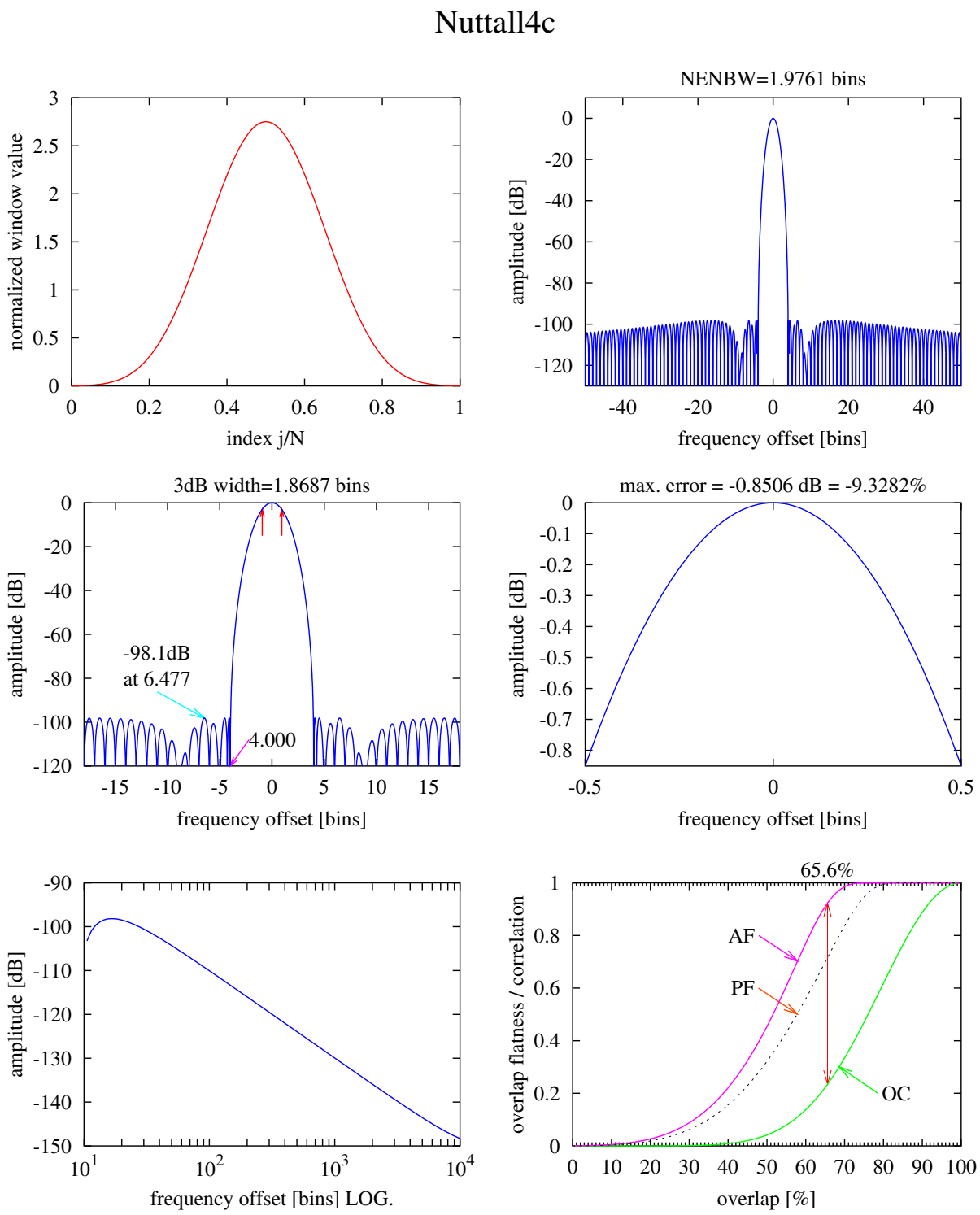

Figure 27 *Nuttall4c window. See text Section C.7.7 on page 36.*

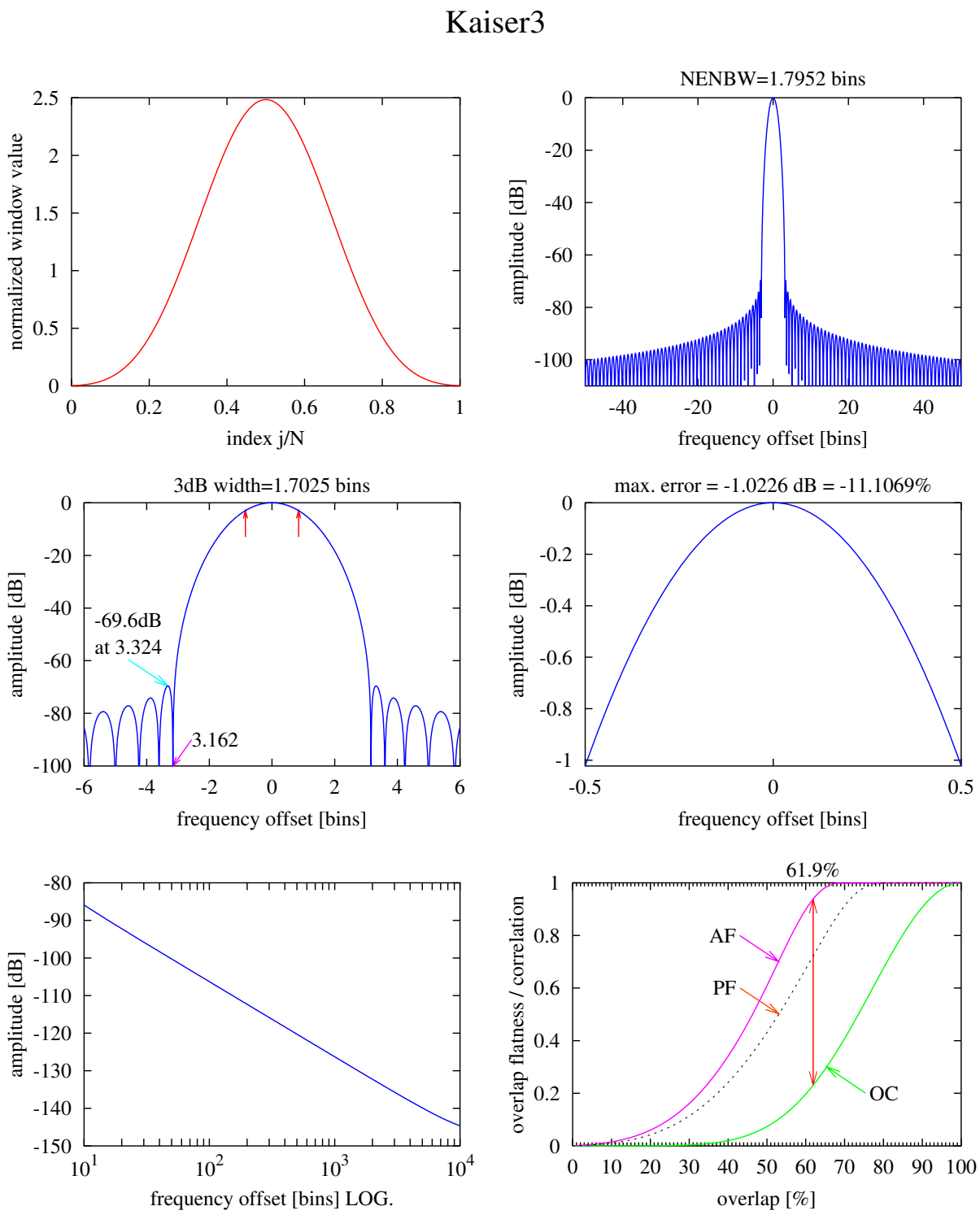

Figure 28 *Kaiser window with $\alpha = 3$. See text Section C.8 on page 36.*

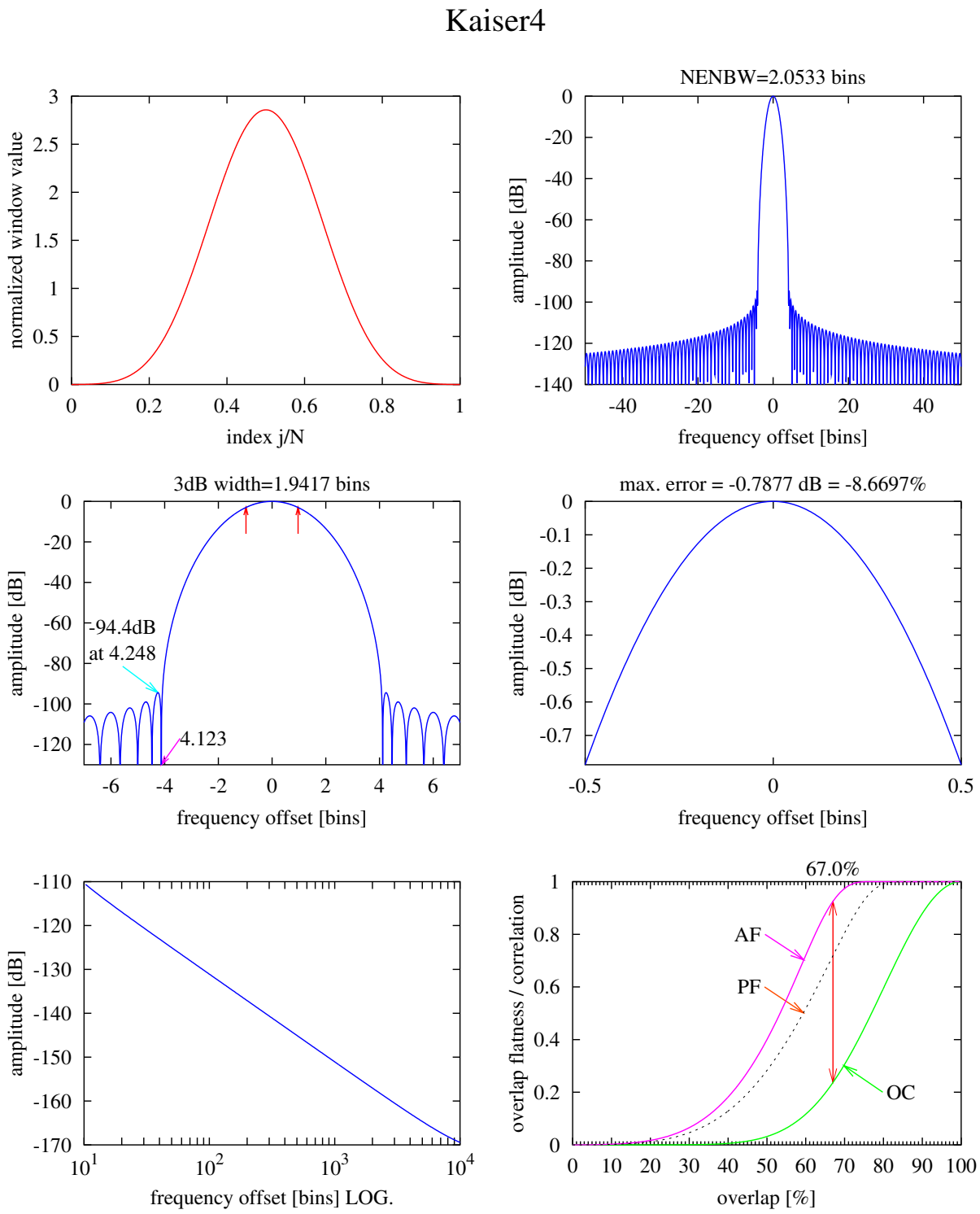

Figure 29 *Kaiser window with $\alpha = 4$. See text Section C.8 on page 36.*

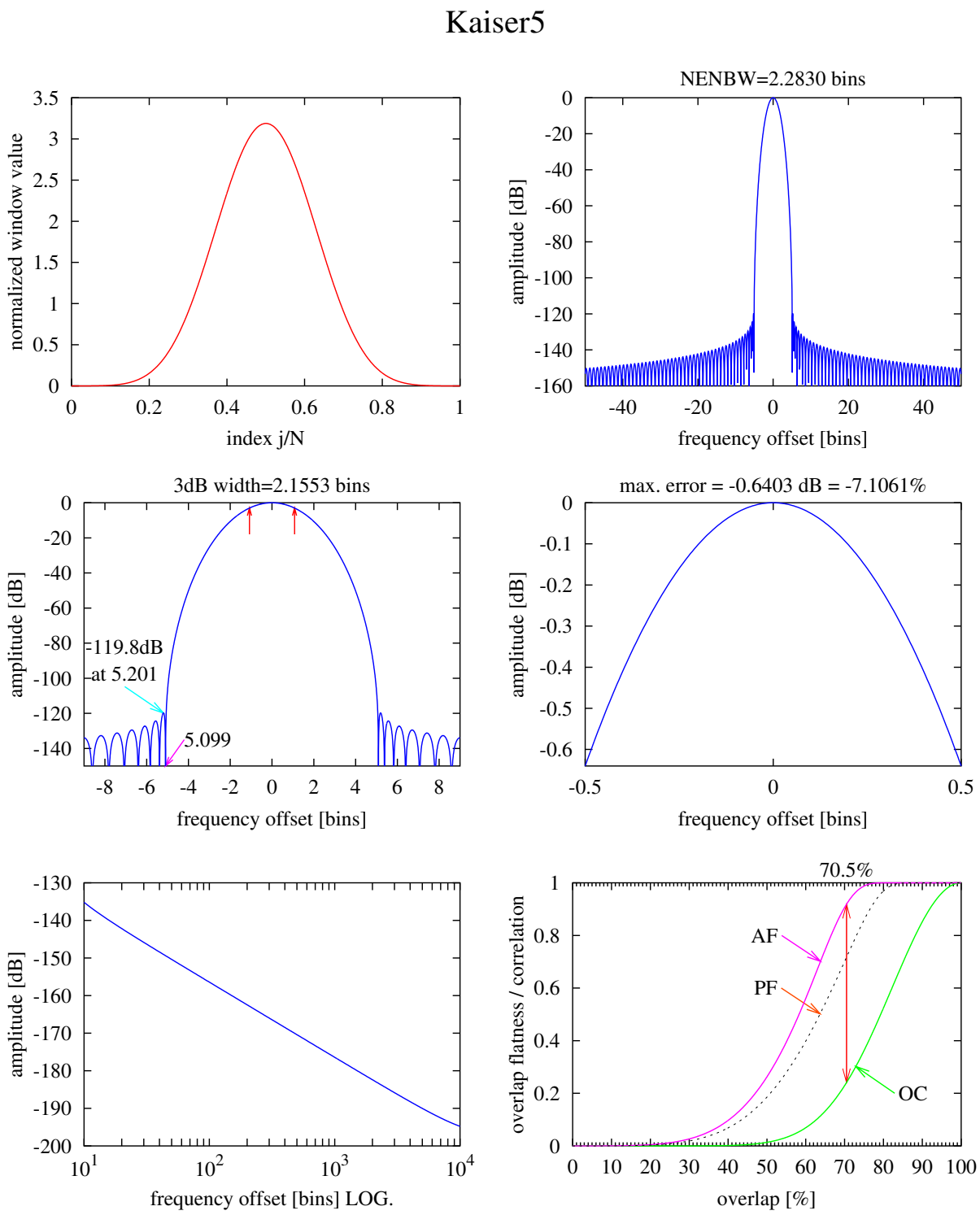

Figure 30 *Kaiser window with $\alpha = 5$. See text Section C.8 on page 36.*

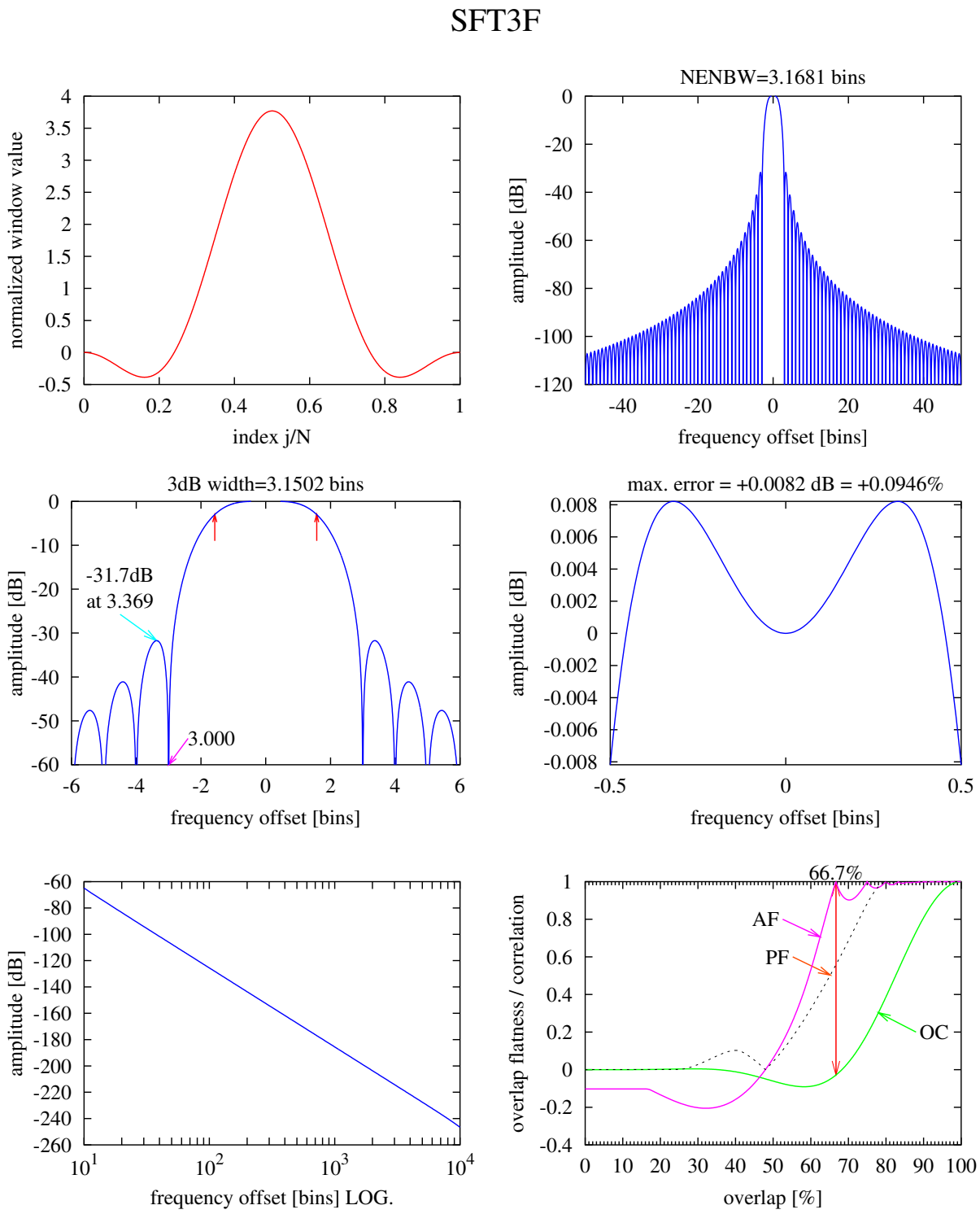

Figure 31 *Fast decaying 3-term flat top window. See text Section D.1 on page 39.*

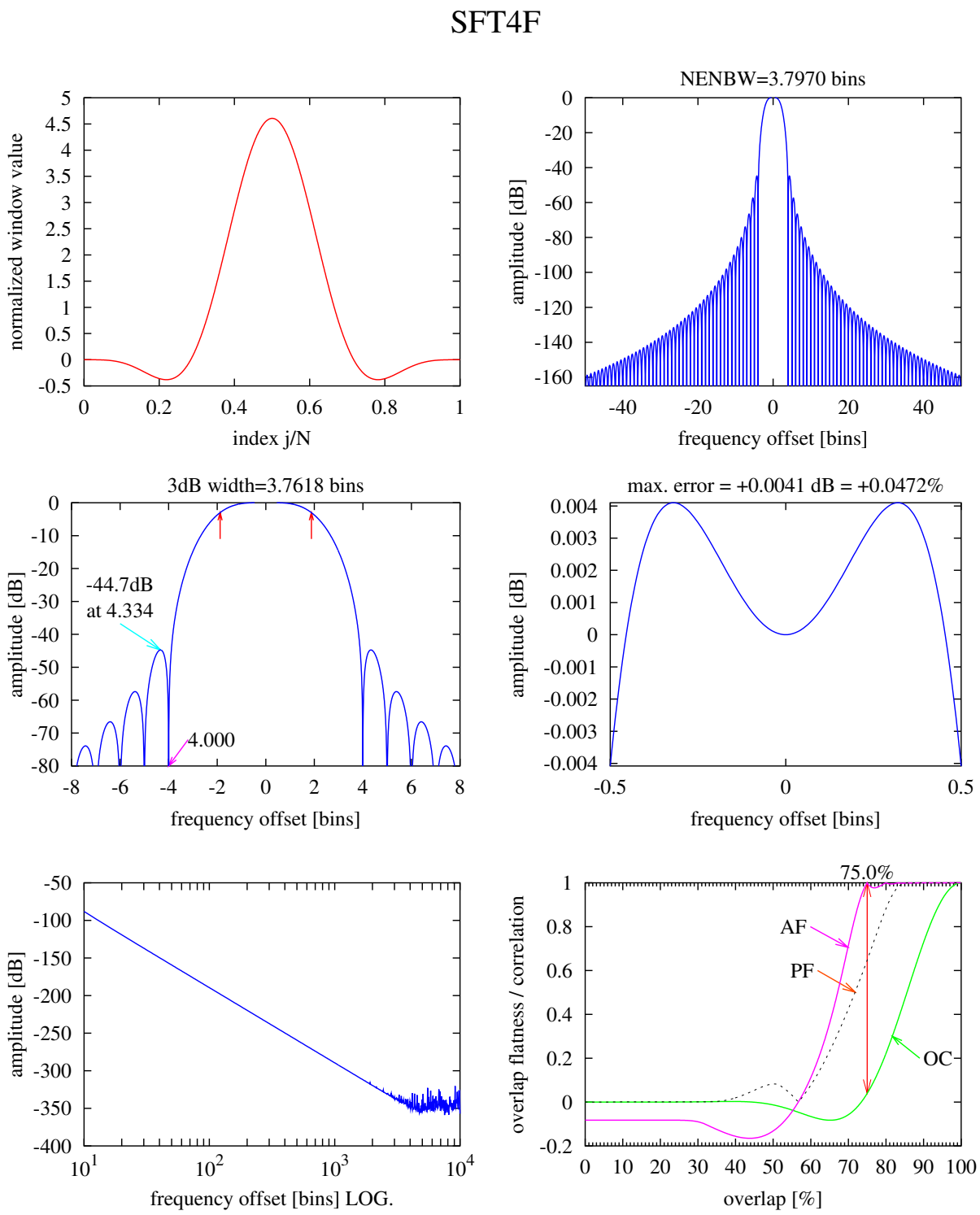

Figure 32 *Fast decaying 4-term flat top window. See text Section D.1 on page 39.*

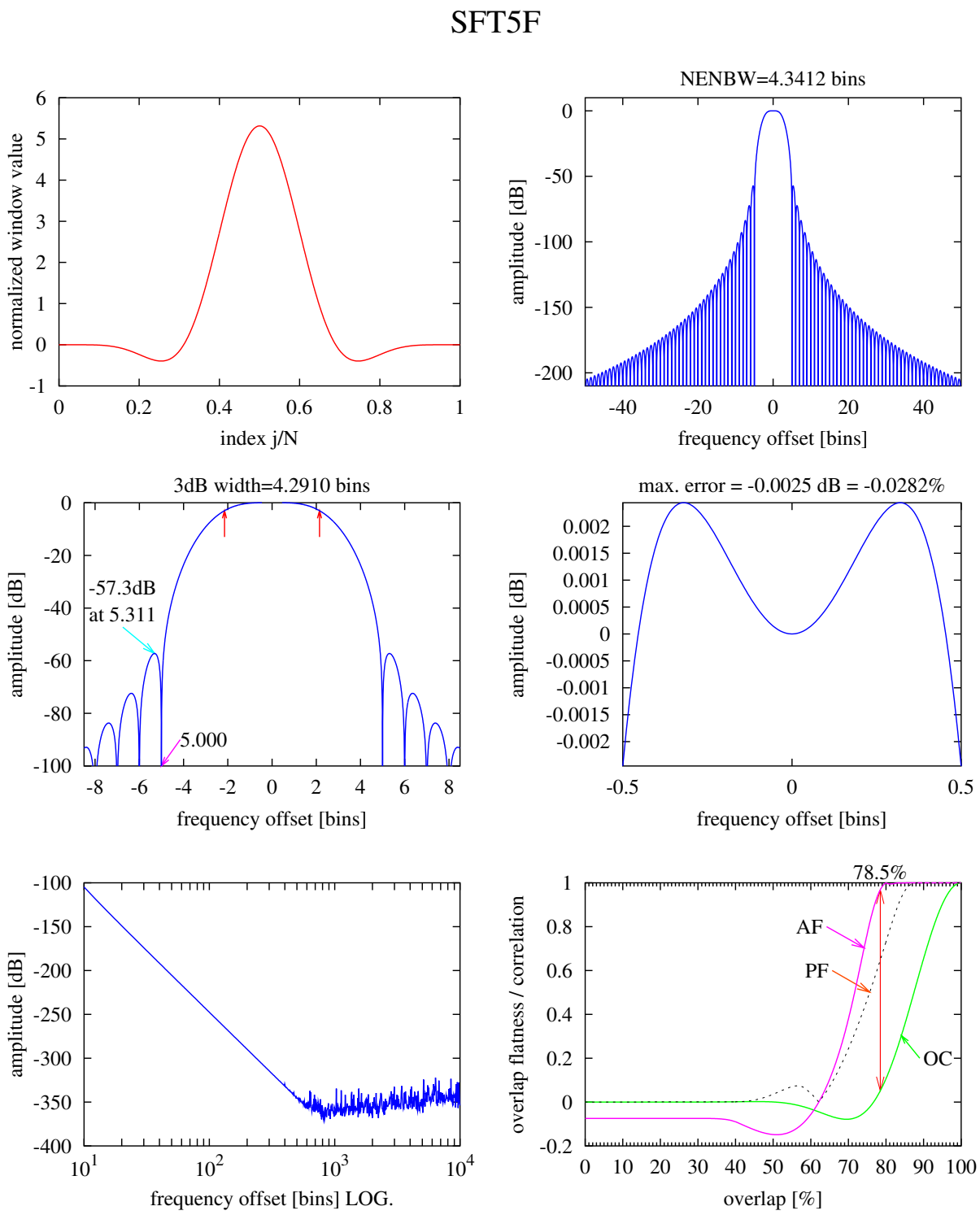

Figure 33 *Fast decaying 5-term flat top window. See text Section D.1 on page 39.*

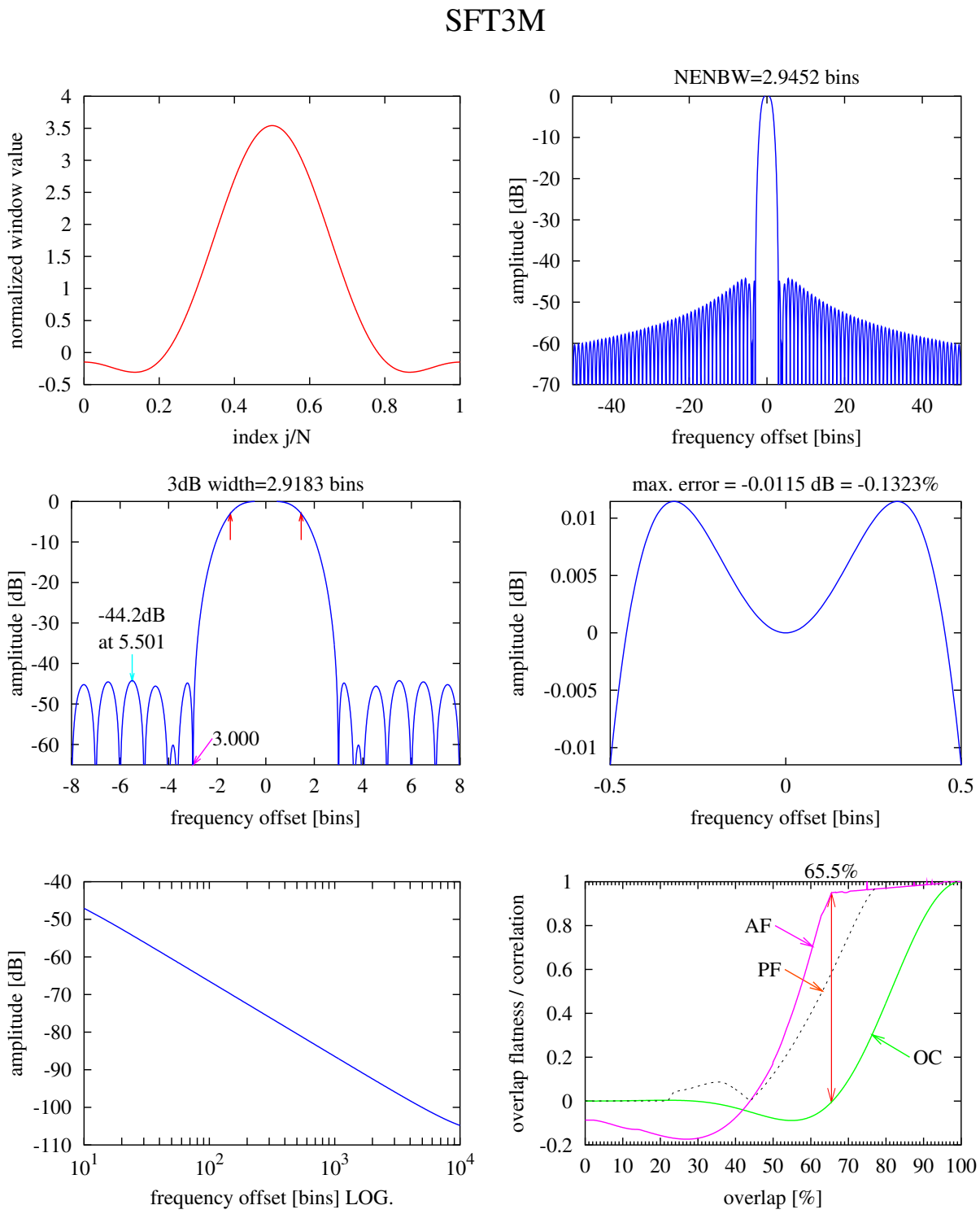

Figure 34 *Minimum sidelobe 3-term flat top window. See text Section D.1 on page 39.*

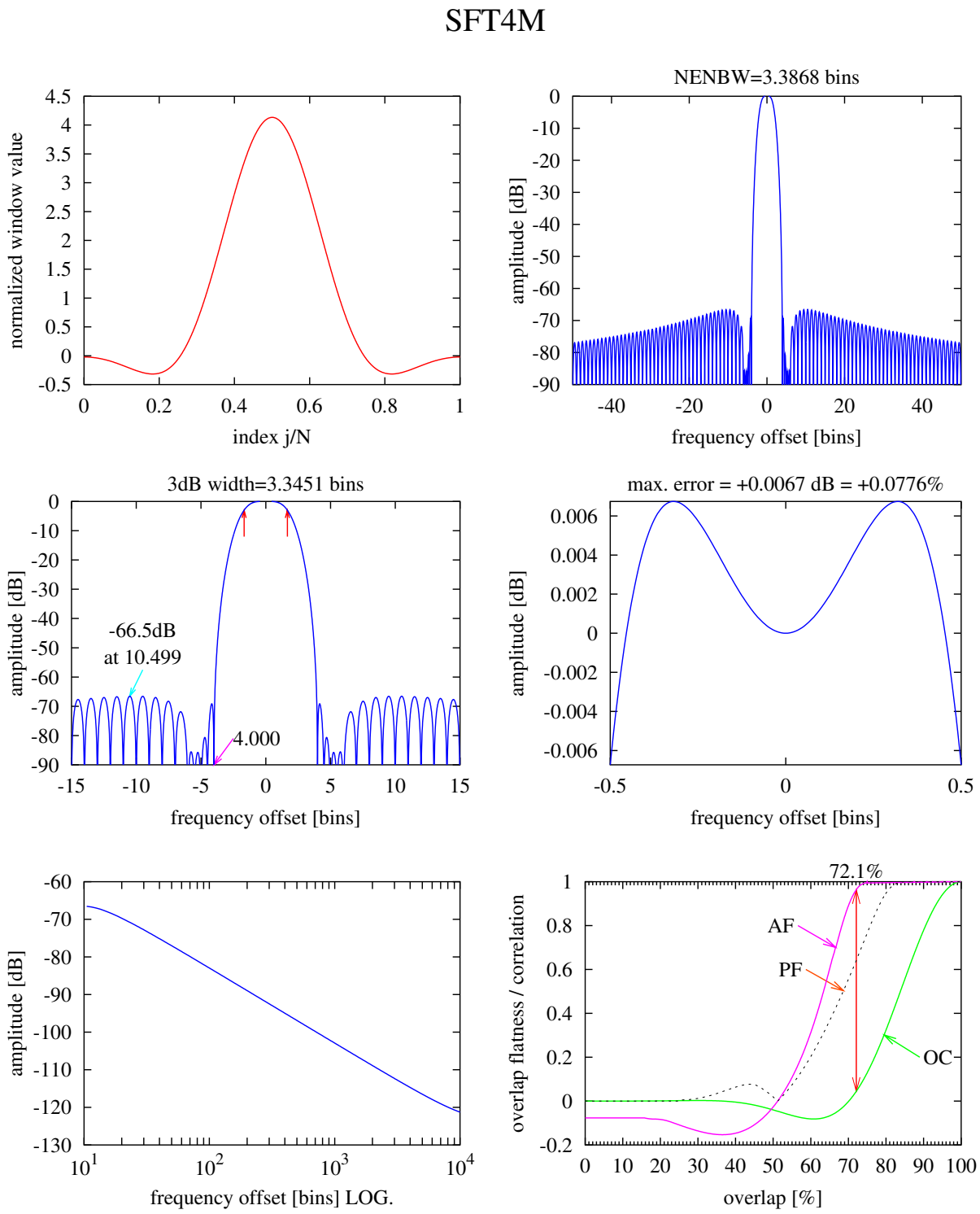

Figure 35 *Minimum sidelobe 4-term flat top window. See text Section D.1 on page 39.*

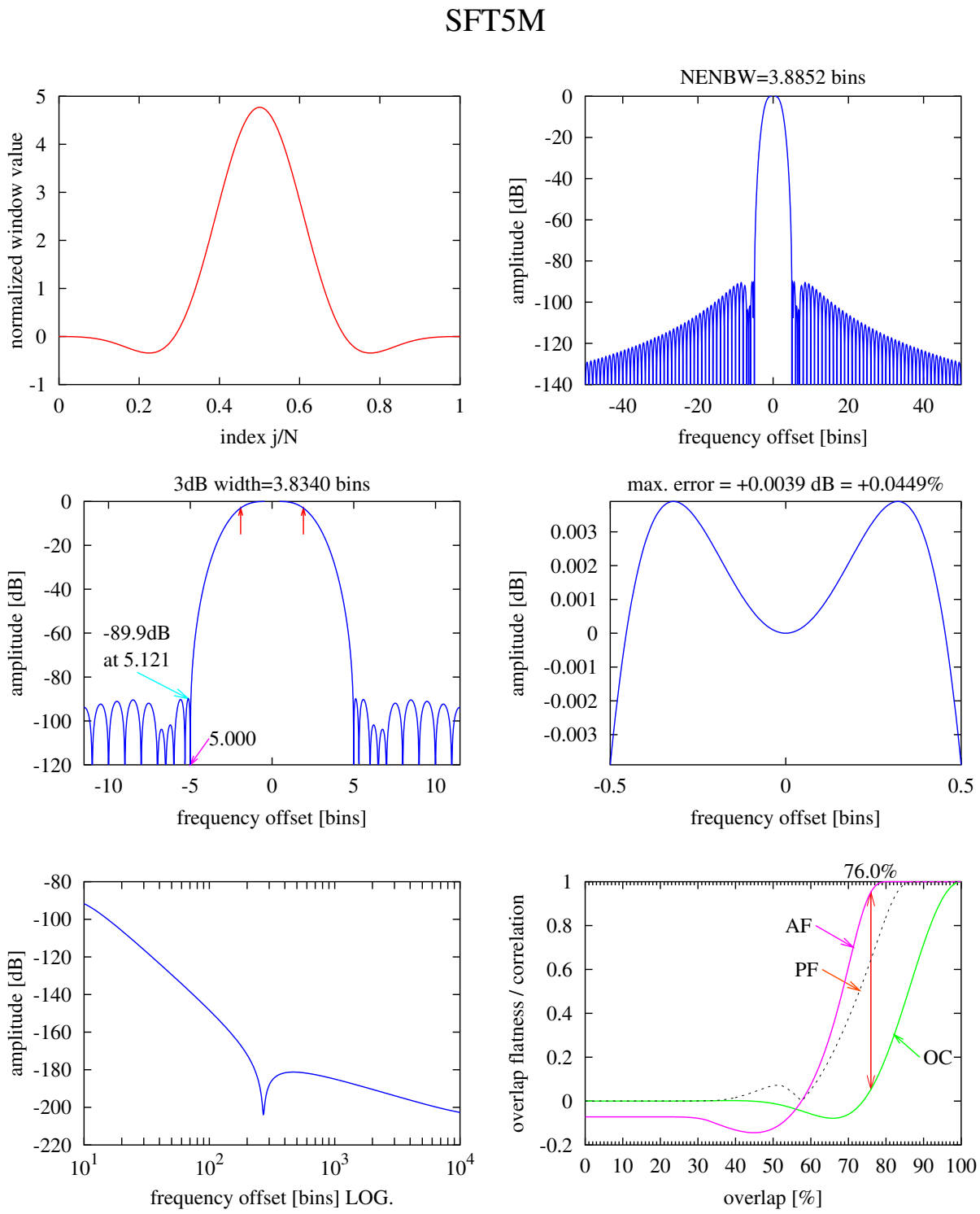

Figure 36 *Minimum sidelobe 5-term flat top window. See text Section D.1 on page 39.*

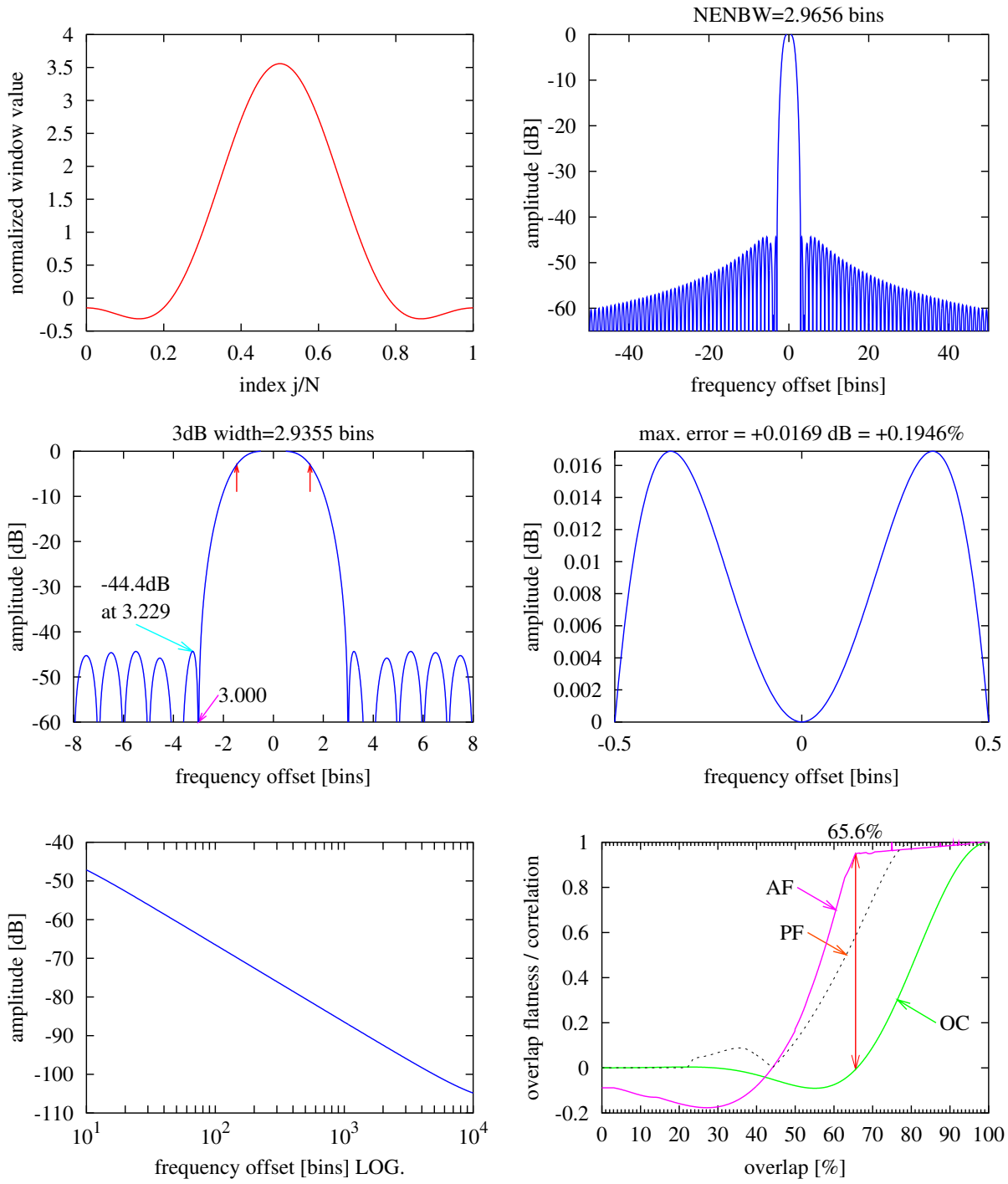

Figure 37 *Flat top window as described by National Instruments. See text Section D.2.1 on page 42.*

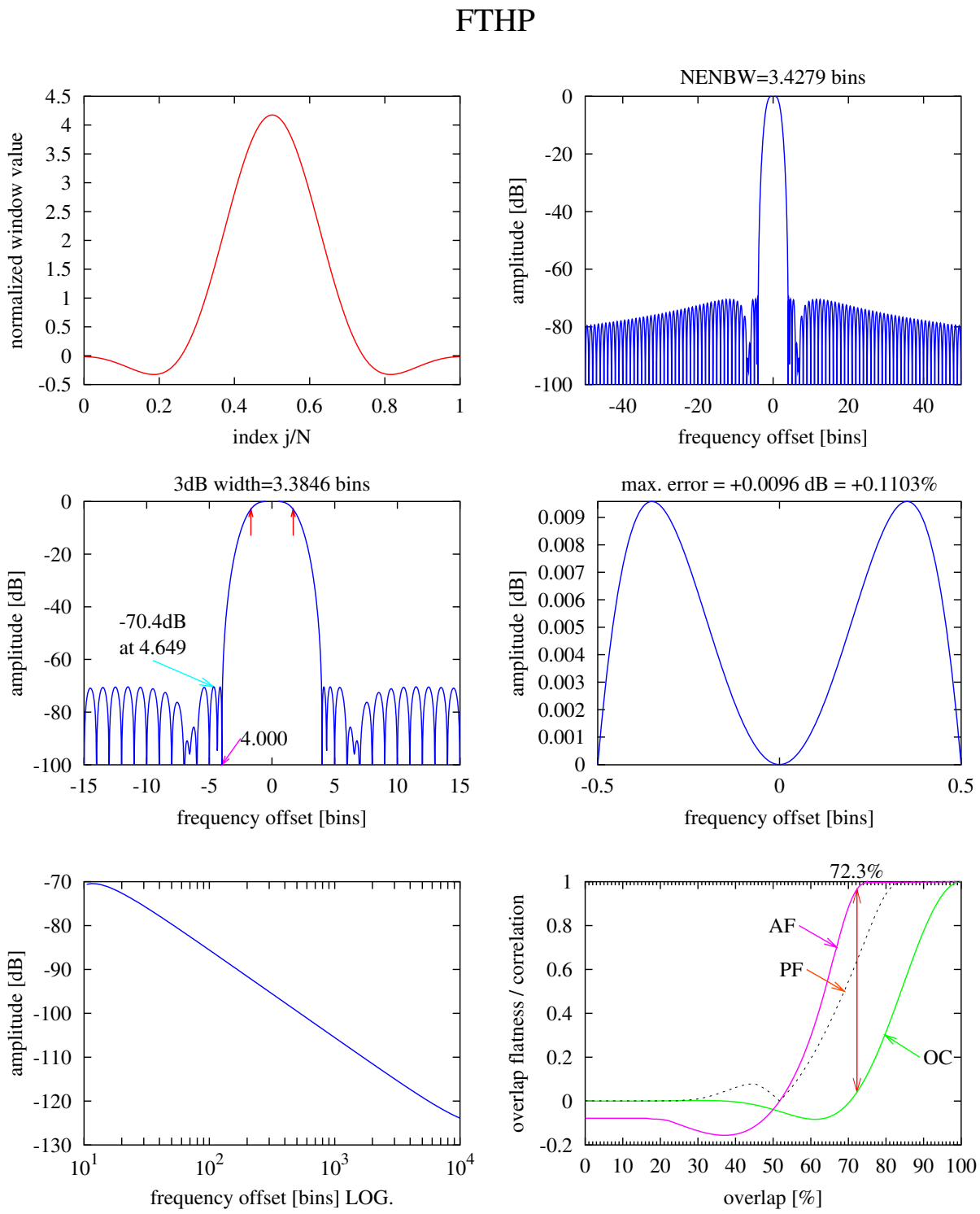

Figure 38 *Flat top window used in older HP spectrum analyzers. See text Section D.2.2 on page 42.*

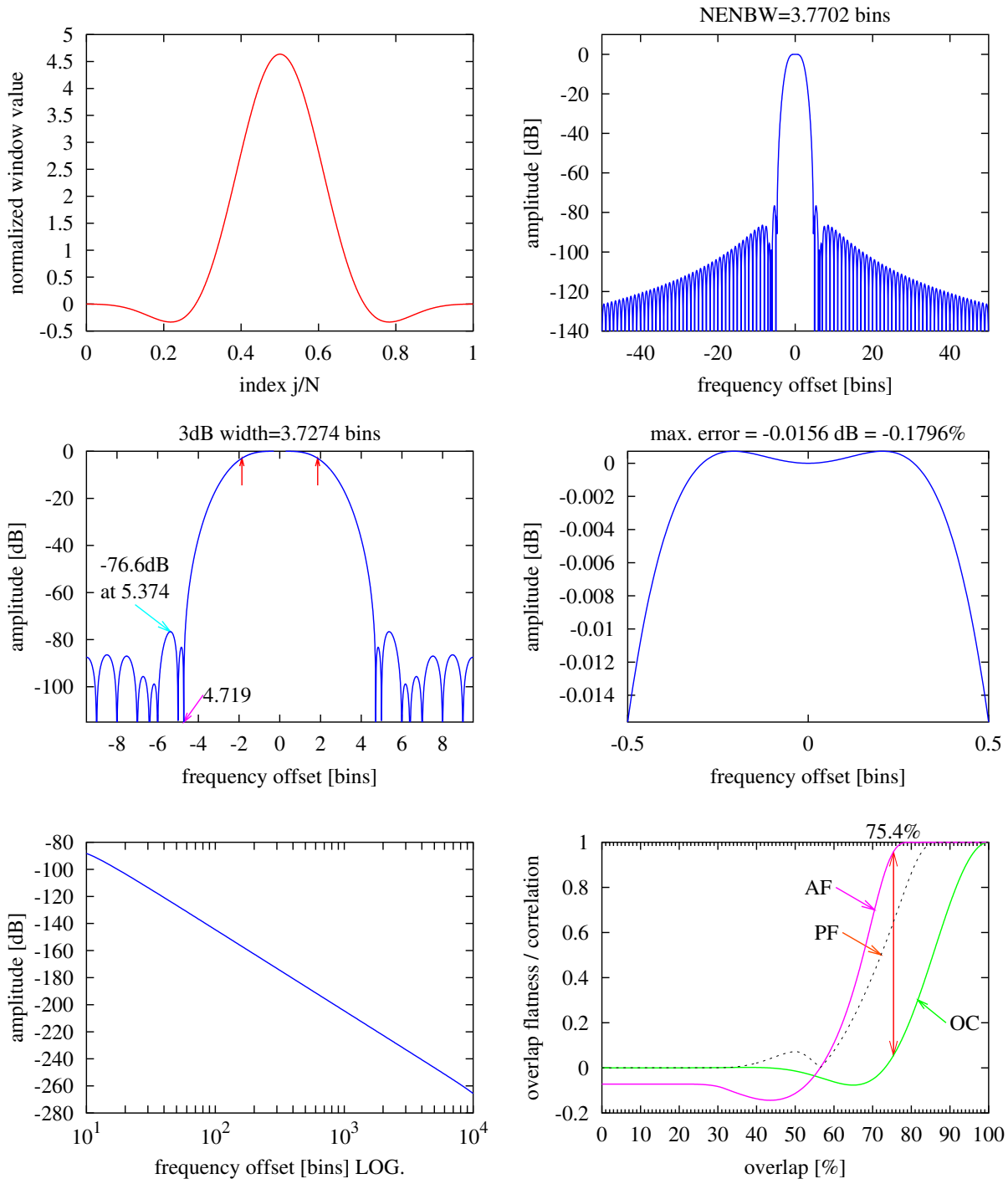

Figure 39 *Flat top window used in the Stanford SR785 spectrum analyzer. See text Section D.2.4 on page 43.*

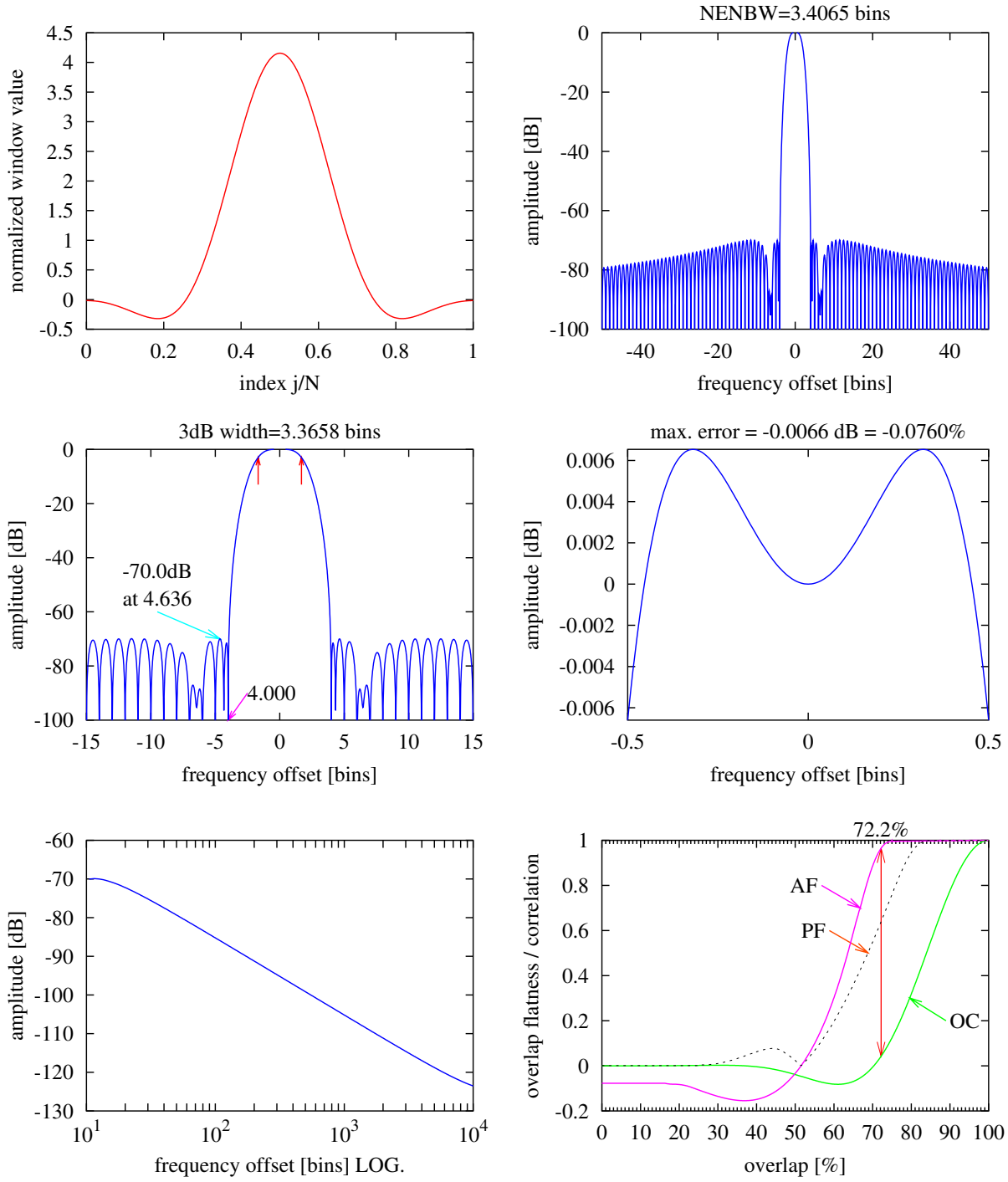

Figure 40 *HFT70 Flat top window. See text Section D.3.1 on page 45.*

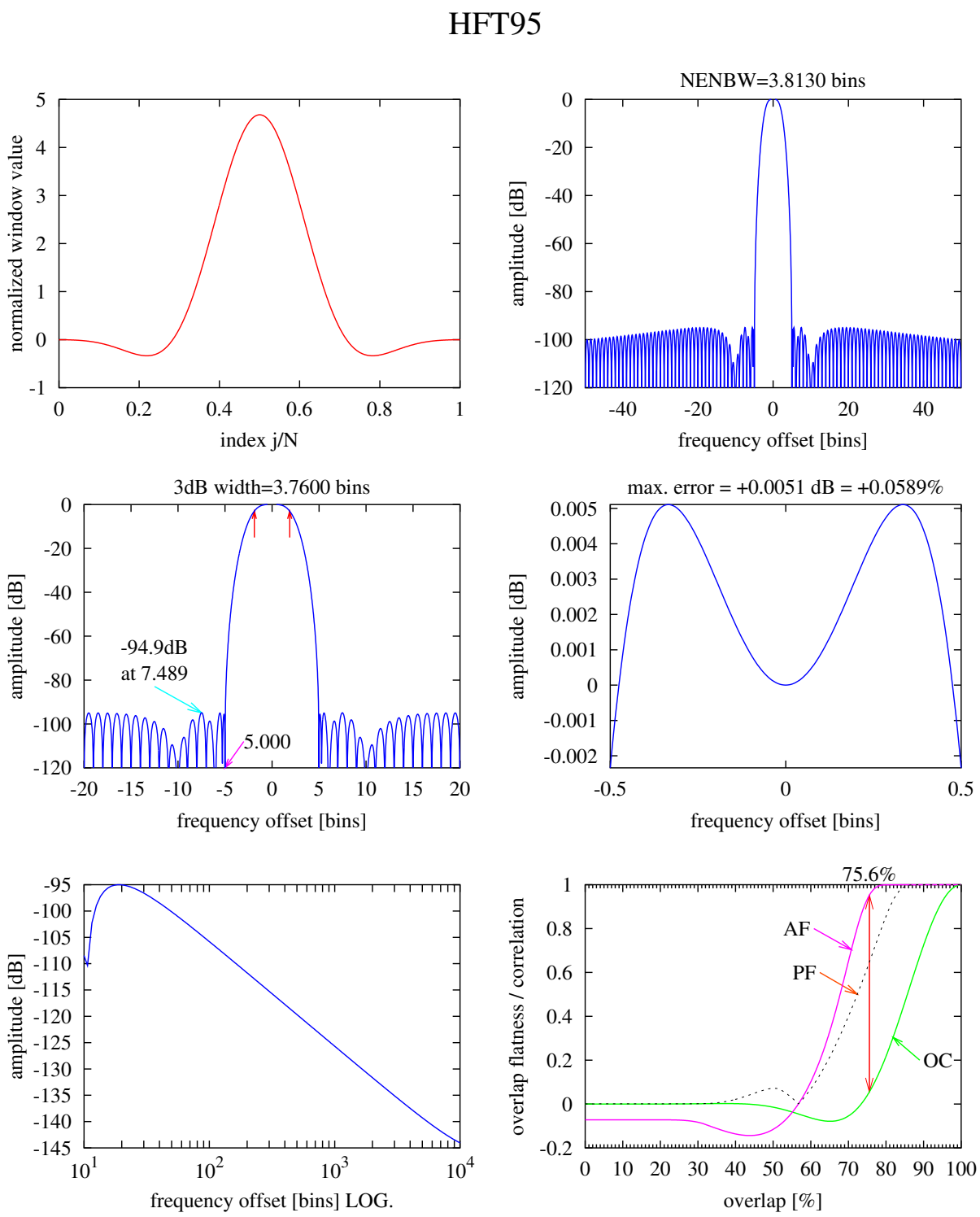

Figure 41 *HFT95 Flat top window. See text Section D.3.2 on page 46.*

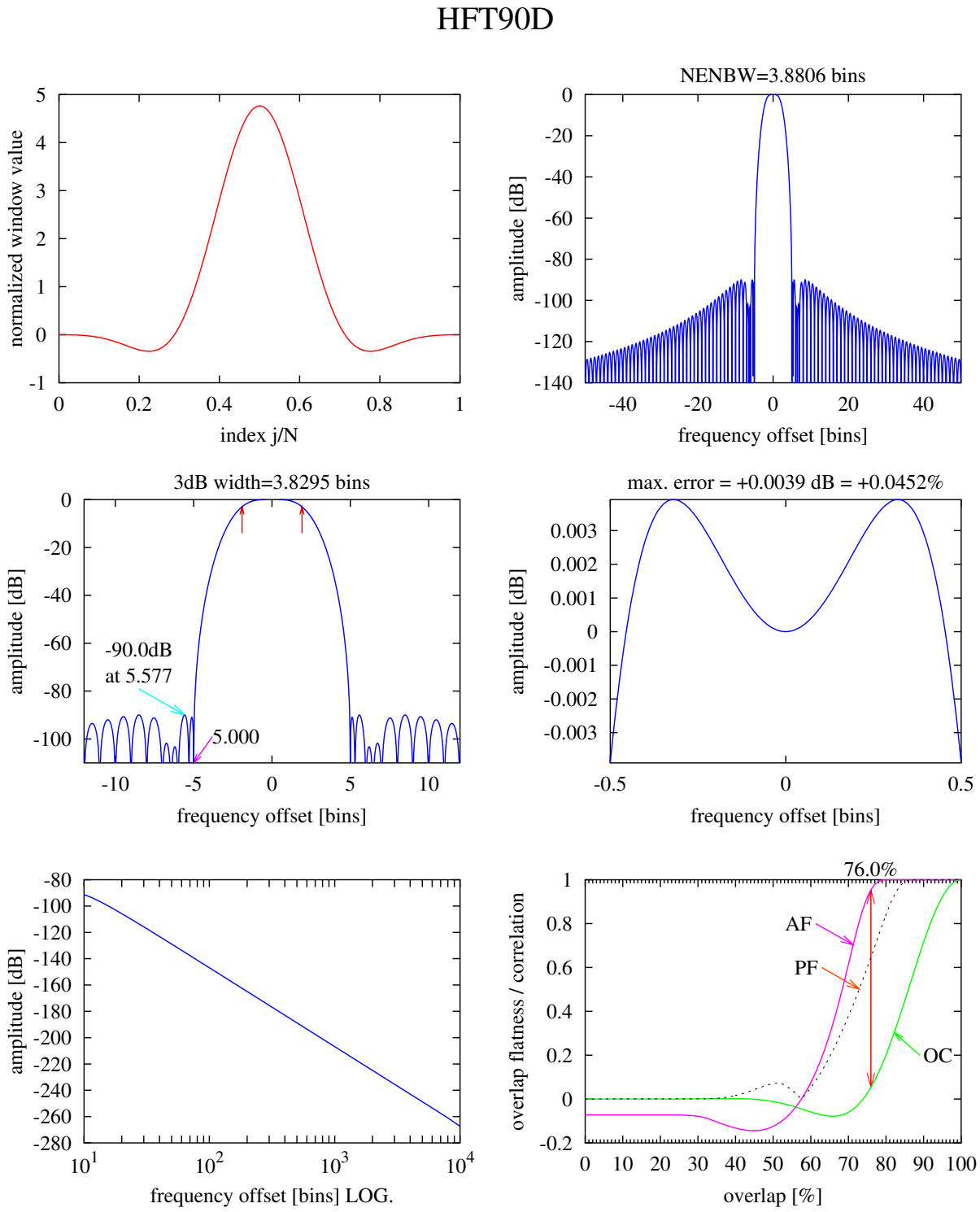

Figure 42 *HFT90D Flat top window. See text Section D.3.3 on page 46.*

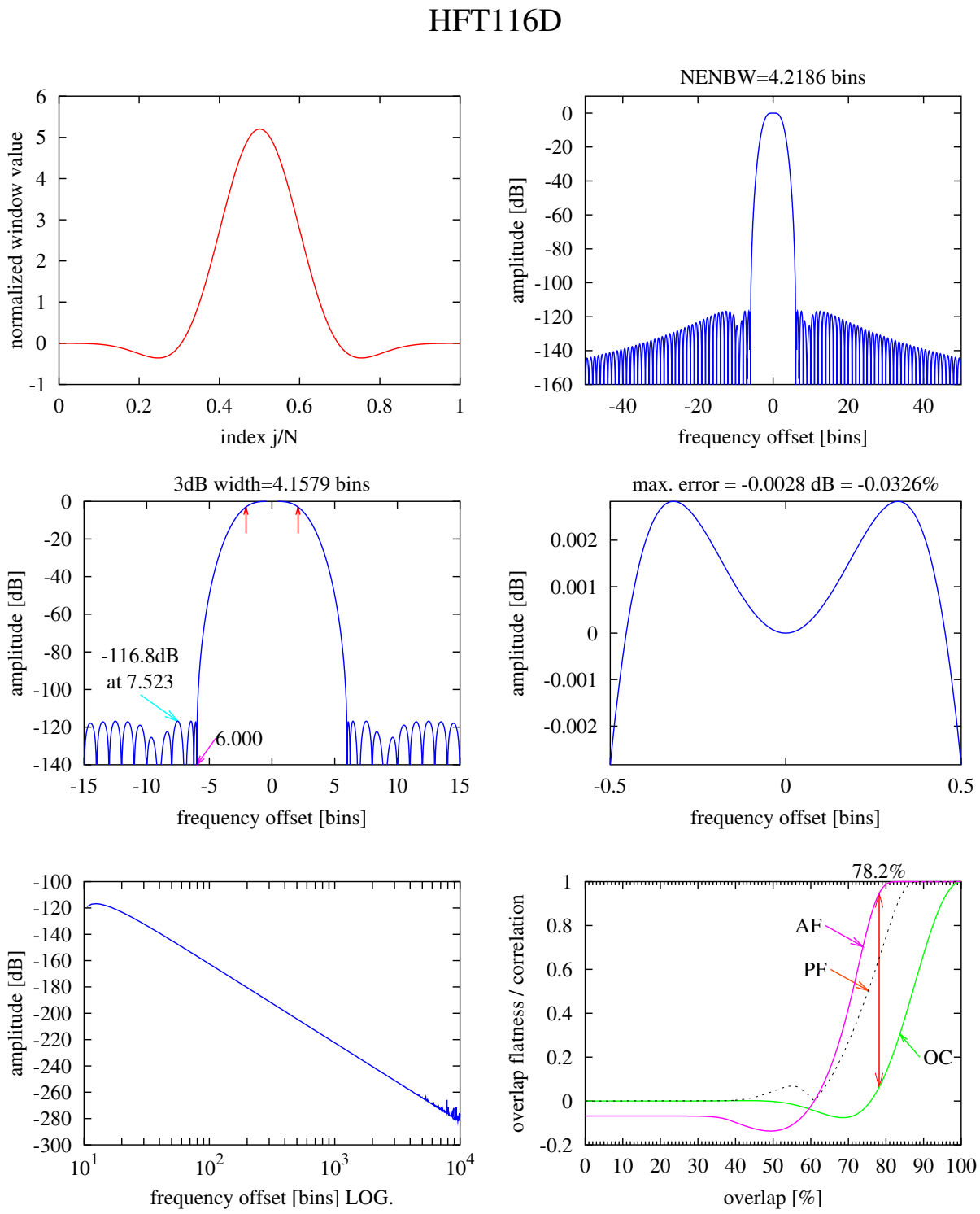

Figure 43 *HFT116D Flat top window. See text Section D.3.4 on page 47.*

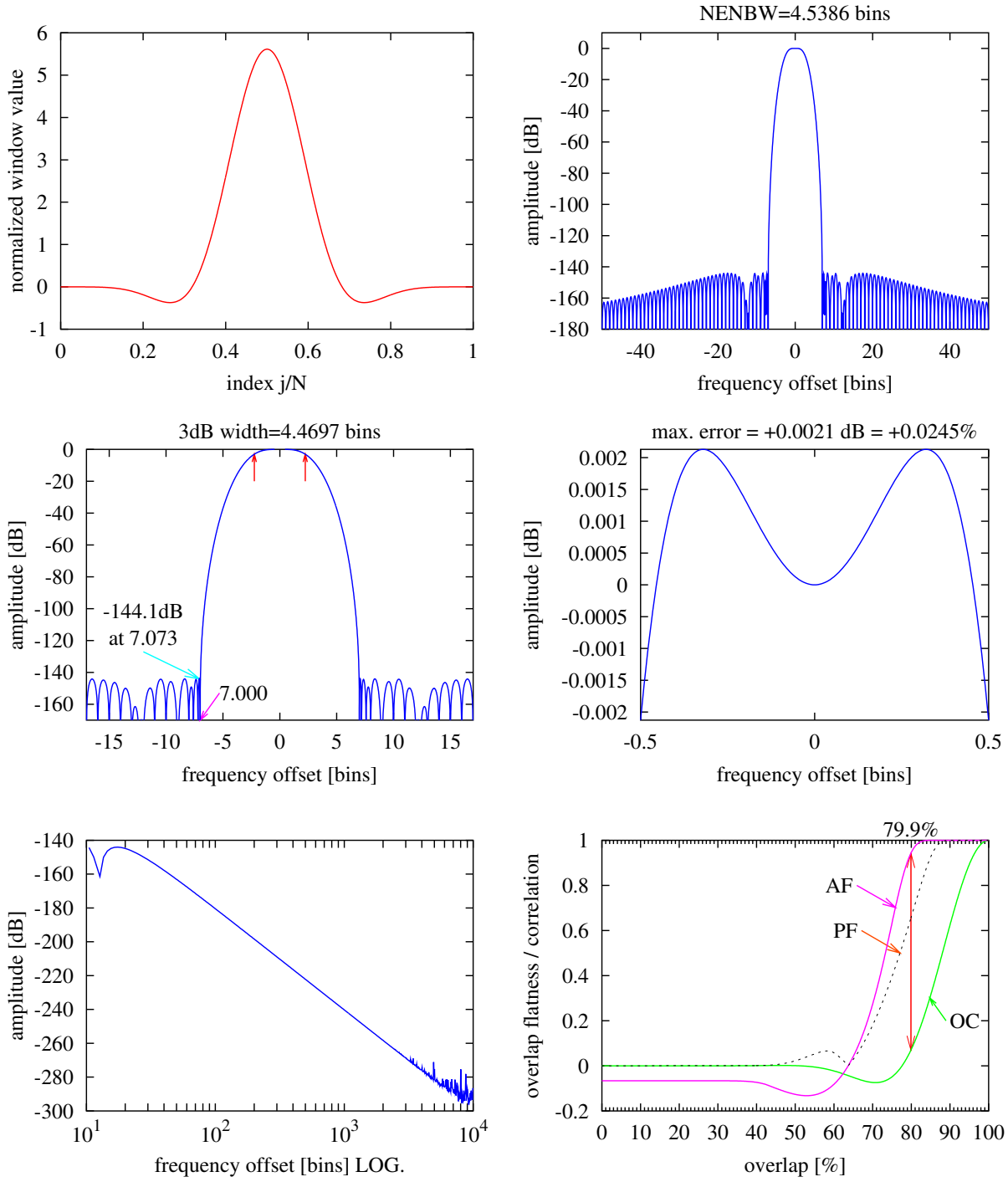

Figure 44 *HFT144D Flat top window. See text Section D.3.5 on page 47.*

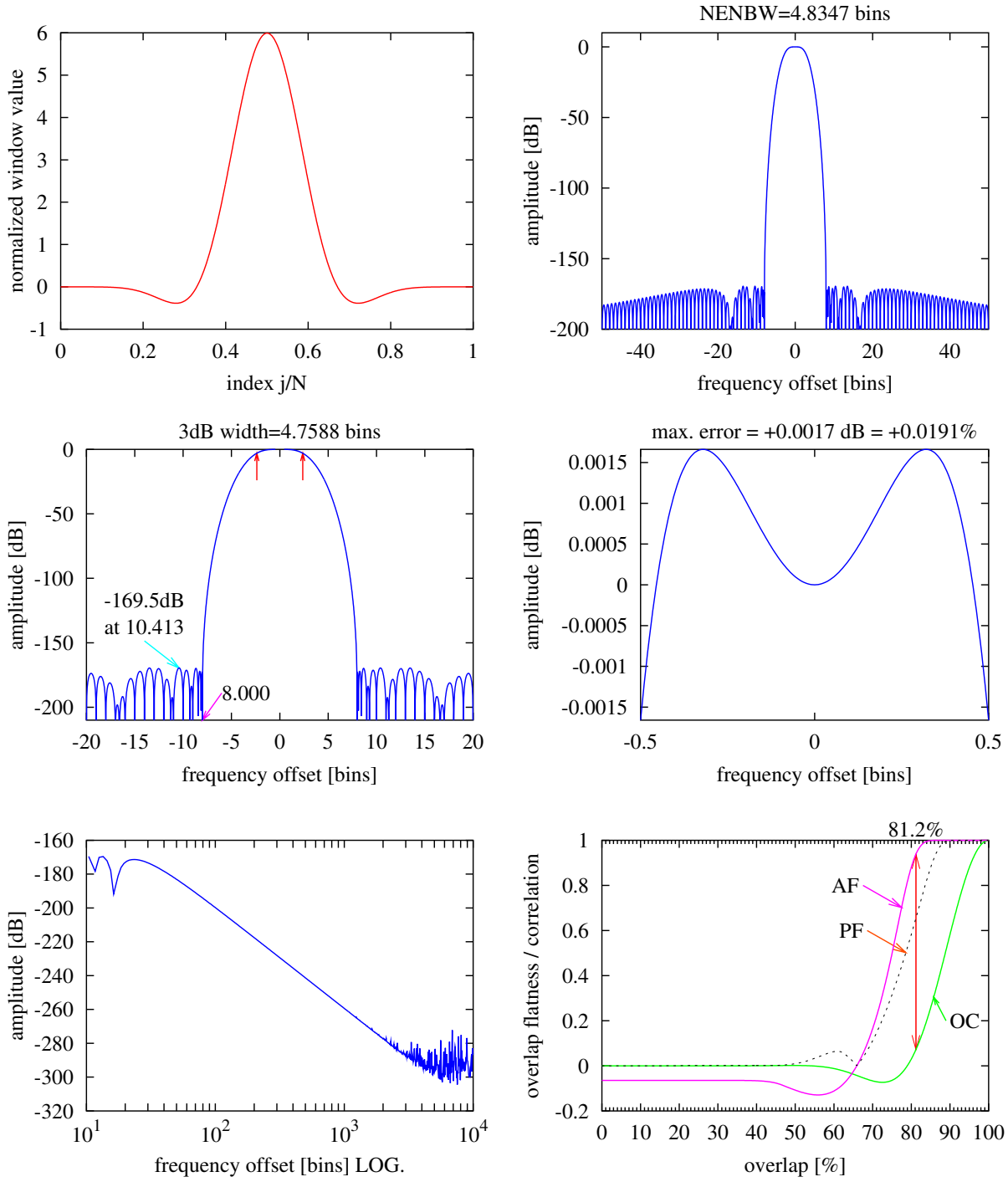

Figure 45 *HFT169D Flat top window. See text Section D.3.6 on page 47.*

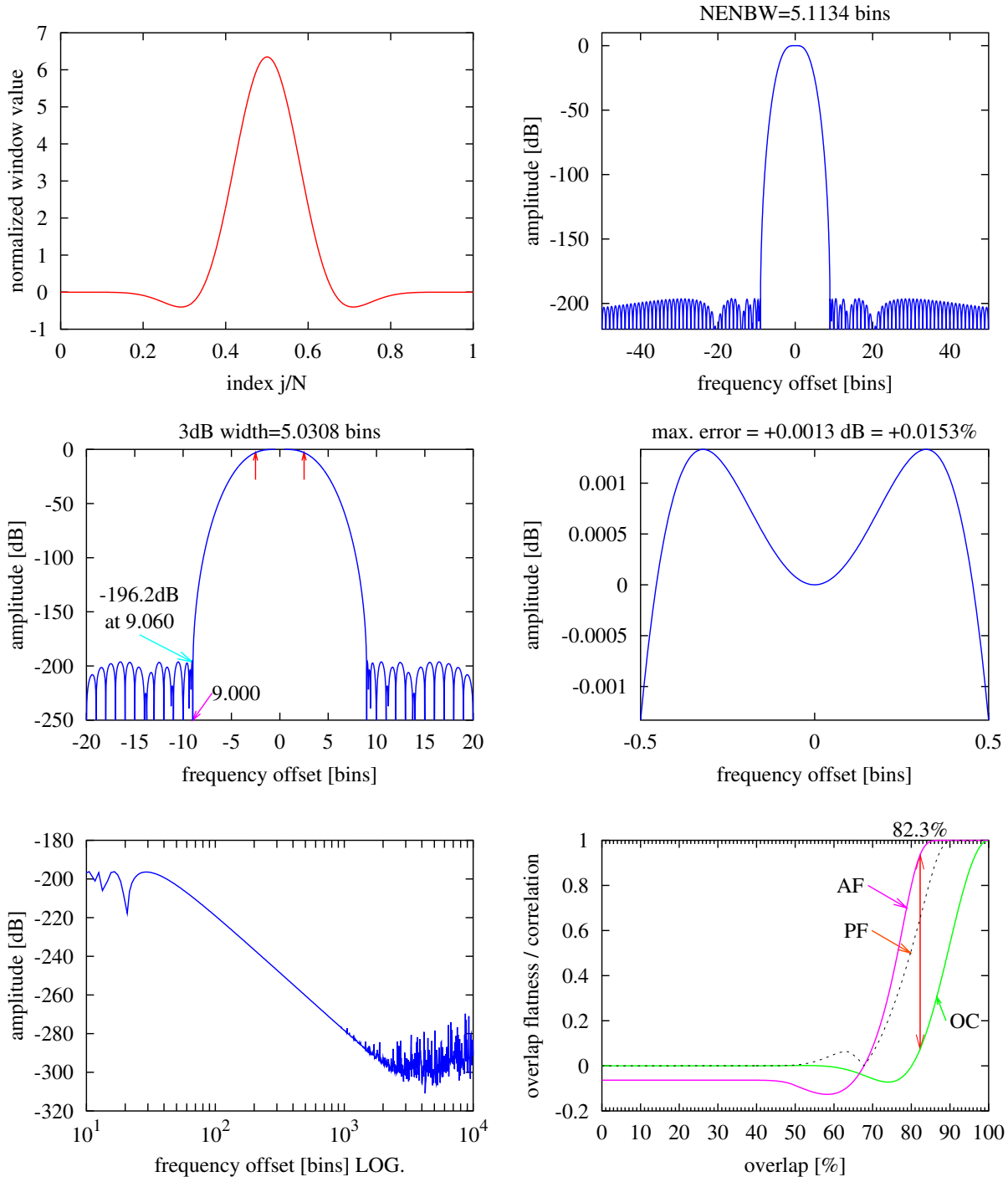

Figure 46 *HFT196D Flat top window. See text Section D.3.7 on page 48.*

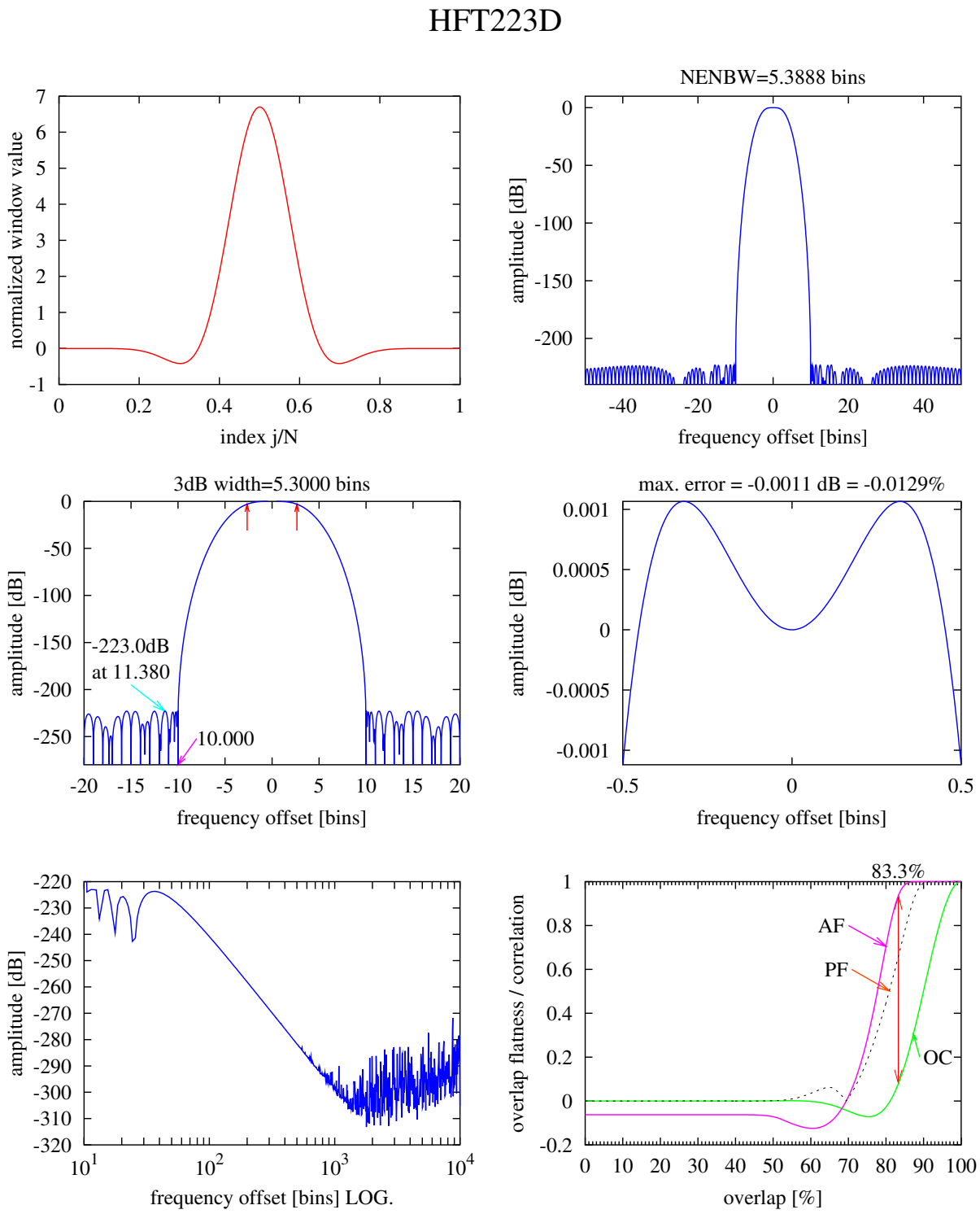

Figure 47 *HFT223D Flat top window. See text Section D.3.8 on page 48.*

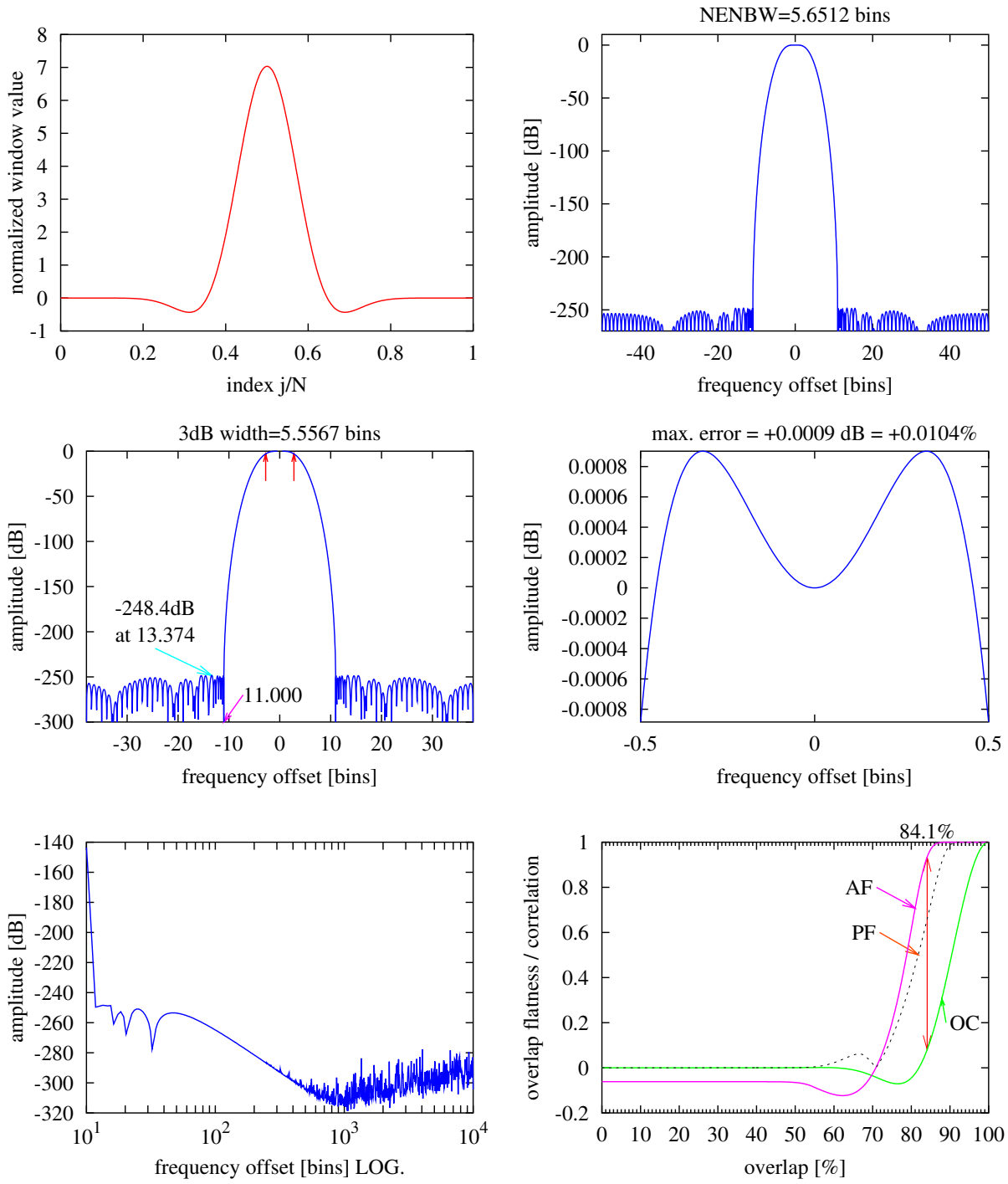

Figure 48 *HFT248D Flat top window. See text Section D.3.9 on page 49.*